Anat Embryol (1994) 190:211–230

Anatomy and Embryology

Original articles

Microscopic structure of the olfactory organ of the clearnose skate, *Raja eglanteria*

Shigeru Takami[1]*, Carl A. Luer[2], Pasquale P. C. Graziadei[1]

[1] Department of Biological Science, B-221, Florida State University, Tallahassee, FL 32306–3050, USA
[2] Mote Marine Laboratory, Sarasota, FL 34236, USA

Accepted: 4 April 1994

Abstract. The olfactory organ of juvenile clearnose skates (*Raja eglanteria*) was studied with the light and electron microscopes. The organ is ovoid in shape, and its free surface is complicated by the presence of some 20 lamellae. Each lamella has a folded surface lined by a typical neurosensory olfactory epithelium. Bipolar olfactory receptor neurons, ciliated sustentacular cells, and basal cells are the pre-eminent cellular components of the epithelium. Two types of receptor neurons, both bearing microvilli but not cilia, were identified. The type 1 neuron is similar to that previously described in other fishes. The type 2 neuron has a characteristic morphology justifying a separate description. Its dendritic knob is larger than that of type 1, and its microvilli, which are shorter and thicker, are straight and regularly arranged. Tight bundles of filaments provide a skeleton to each microvillus, and these filament bundles reach more than 5 μm down into the dendrite. Type 2 receptor neurons have a well-developed Golgi complex and sparse rough endoplasmic reticulum (rER), whereas type 1 receptor neurons have a less well-developed Golgi complex and a conspicuous sytem of rER lamellae. The mucous layer on the epithelial surface is provided by the secretion of goblet cells that are situated mostly in the peripheral regions of each lamella. Secretory granules in the sustentacular cells and glands in the lamina propria were not observed.

Key words: Olfactory epithelium – Olfactory receptor neurons – Skate olfactory system – Sustentacular cells – Goblet cells

Introduction

The first-order neurons of the vertebrate olfactory system, olfactory receptor neurons, are bipolar neuroepithelial cells present in the olfactory epithelium (OE) of the nasal cavity. Each olfactory receptor neuron sends a single, unbranched dendrite to the epithelial surface, where it terminates in a "dendritic knob" provided with cilia and/or microvili, the presumed sites of odor-stimulus reception (Getchell 1986; Anholt 1987). An axon, originating from the base of the cell soma, projects to the superficial layer of the olfactory bulb (OB), where it intermingles with others, forming a plexiform structure, and then terminates in characteristic glomeruli. In these glomeruli the sensory axons synapse with the branches of the mitral cell dendrites (for reviews, see Graziadei 1973, 1977, 1990; Getchell 1986; Lancet 1986; Anholt 1987).

Morphological observations of olfactory receptor neurons have been reported in many fish species, and at least in teleosts, both ciliated and microvillar olfactory receptor neurons have been reported (for review, see Eisthen 1992). In several chondrichthian fishes, however, only microvillar receptor neurons have so far been described (Reese and Brightman 1970; Holl 1973; Bronshtein 1976; Theisen et al. 1986; Zeiske et al. 1986).

Recently, Luer and Gilbert (1985) have succeeded in mating, hatching, and rearing the clearnose skate, *Raja eglanteria*, in the laboratory. The embryos develop in their egg cases for 11–13 weeks before hatching. These embryos can be removed from their egg cases, experimentally manipulated, and then returned to controlled seawater conditions to survive until hatching (Luer 1989). We have studied the trophic interaction between the nose and the CNS olfactory centers in neonatal and adult mammals, as well as in amphibia (Stout and Graziadei 1980; Monti Graziadei and Graziadei 1984; Magrassi and Graziadei 1985; Graziadei and Monti Graziadei 1985, 1992; Graziadei 1990). Clearnose skates, when developed in the laboratory under controlled conditions, may serve well as a model for studying similar phenomena of trophic interaction between the olfactory organ and the CNS. Consequently, basic knowledge of their olfactory organ could be essential to future studies of experimental neurobiology.

So far only gross anatomical studies have been reported on the olfactory organ (OO) of *Raja* (Meng and Yin 1981). It is the purpose of this paper to investigate the

* *Present address*: Department of Physiology, University of Kentucky College of Medicine, Lexington, KY 40536, USA
Correspondence to: S. Takami

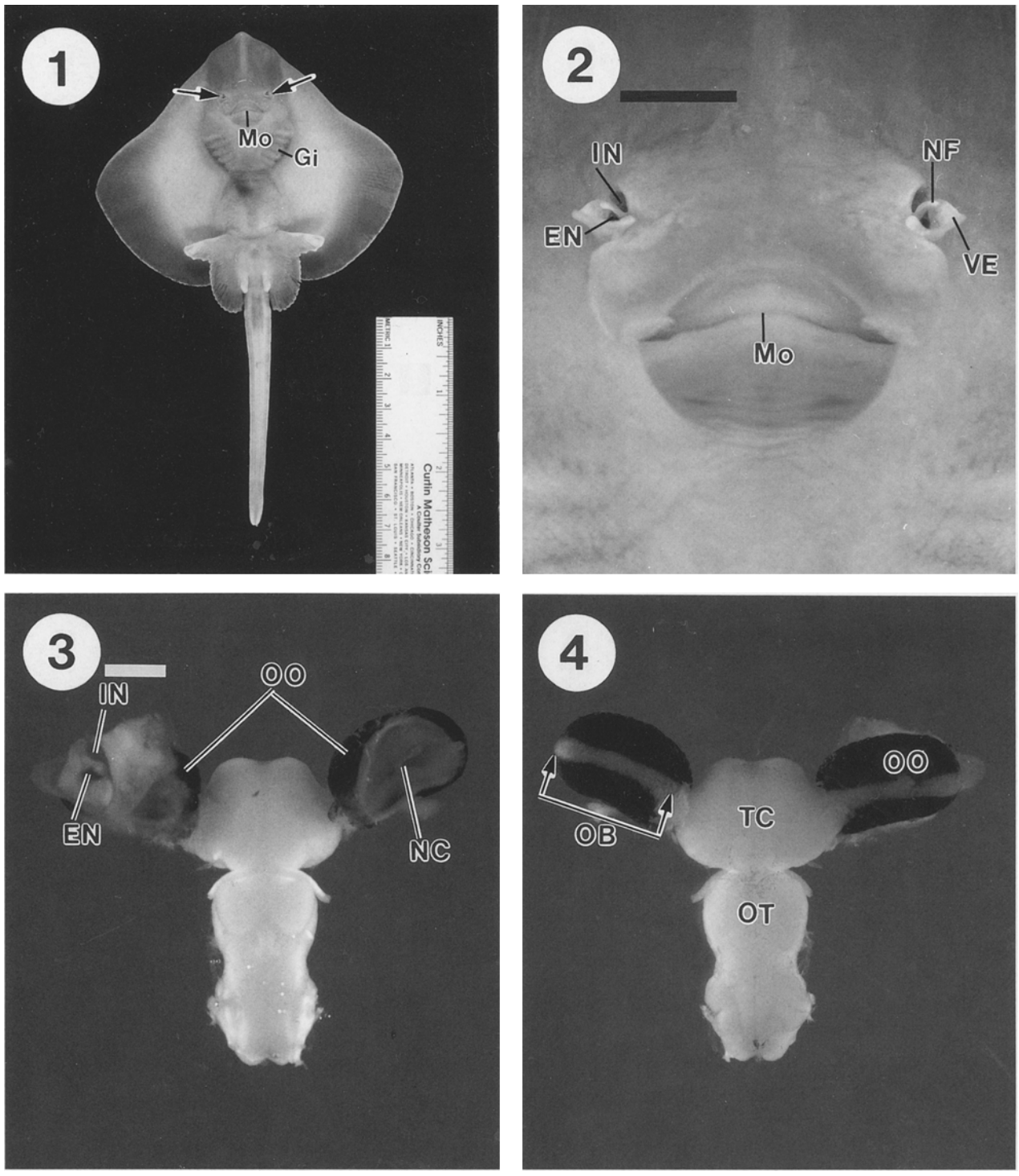

Fig. 1. Ventral view of the whole body of a *juvenile clearnose skate, Raja eglanteria.* Openings of the olfactory organ *(arrows)* are located anterior to the mouth *(Mo). Gi,* Gills. See the ruler for magnification

Fig. 2. Higher magnification of the olfactory openings. They are divided into the anterior incurrent nostril *(IN)* and posterior excurrent nostril *(EN).* These nostrils are incompletely separated via a nasal flap *(NF);* a valvular extension *(VE)* is located along the outer margin of the *EN. Mo,* Mouth. *Bar* 5 mm

Fig. 3. Ventral view of the bilateral olfactory organs *(OO)* and brain. The concave surface of each organ is the nasal cavity *(NC).* Partly dissected right *OO* , at the left, shows that the anterior incurrent and posterior excurrent nostrils *(IN* and *EN,* respectively) are located in the lateral part of the *NC. Bar* 10 mm

Fig. 4. Dorsal view of the *OO,* olfactory bulb *(OB),* telencephalon *(TC),* optic tectum *(OT),* and the rest of the brain. Note that a tubular *OB* is attached on the convex surface of the *OO.* Magnification is the same as in Fig. 3

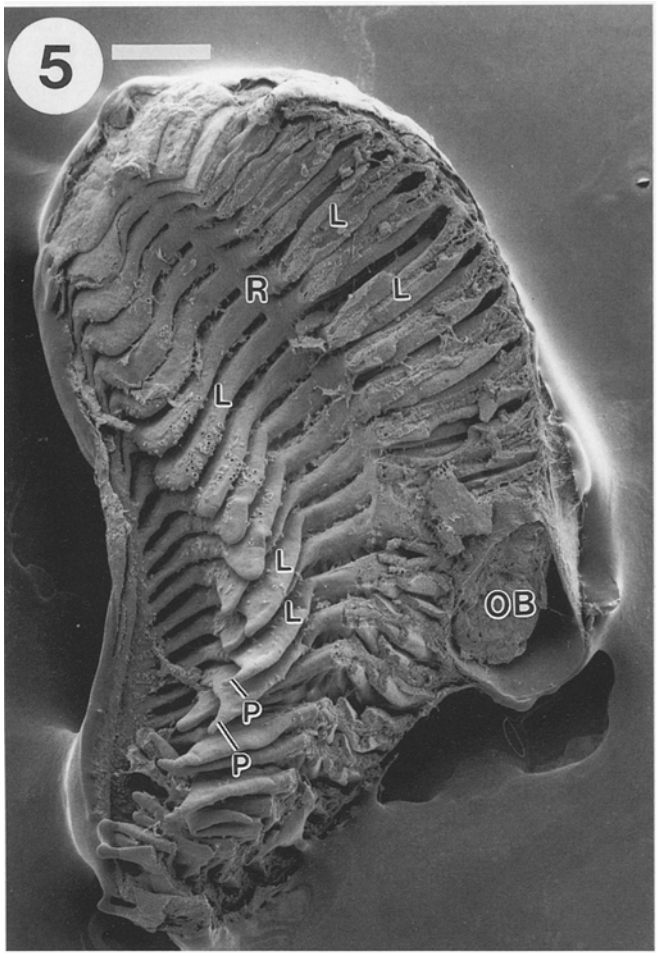
5
L
R
L
L
L
L
OB
P
P

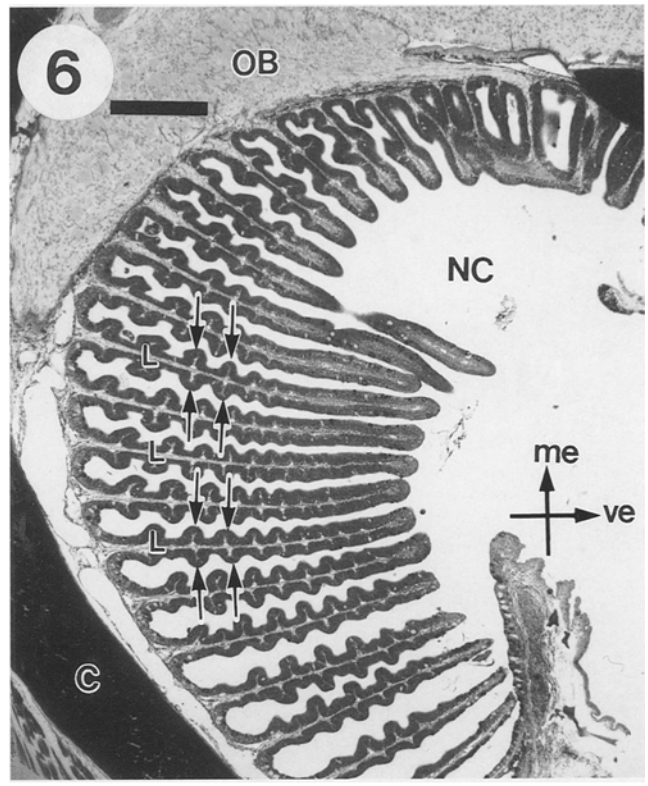
6
OB
NC
L
L
L
me
ve
C

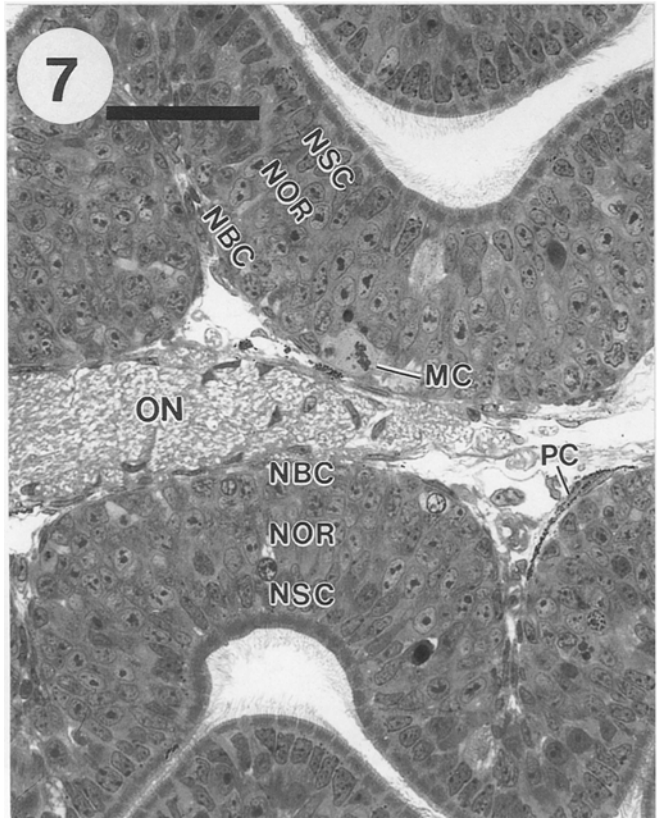
7
NSC
NOR
NBC
MC
ON
PC
NBC
NOR
NSC

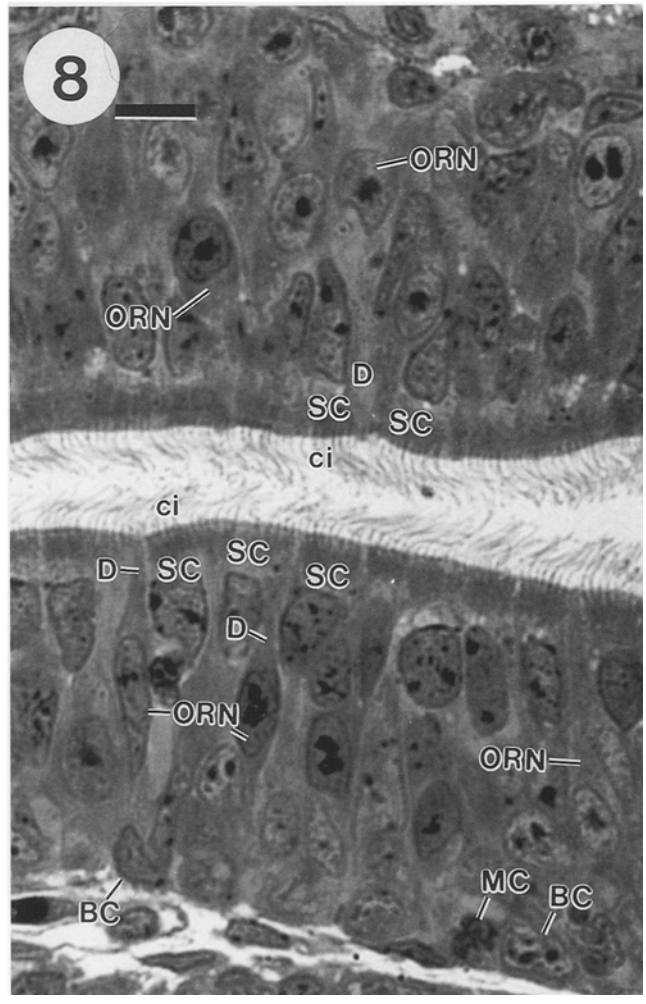
8
ORN
ORN
D
SC
SC
ci
ci
D
SC
SC
SC
D
ORN
ORN
BC
MC
BC

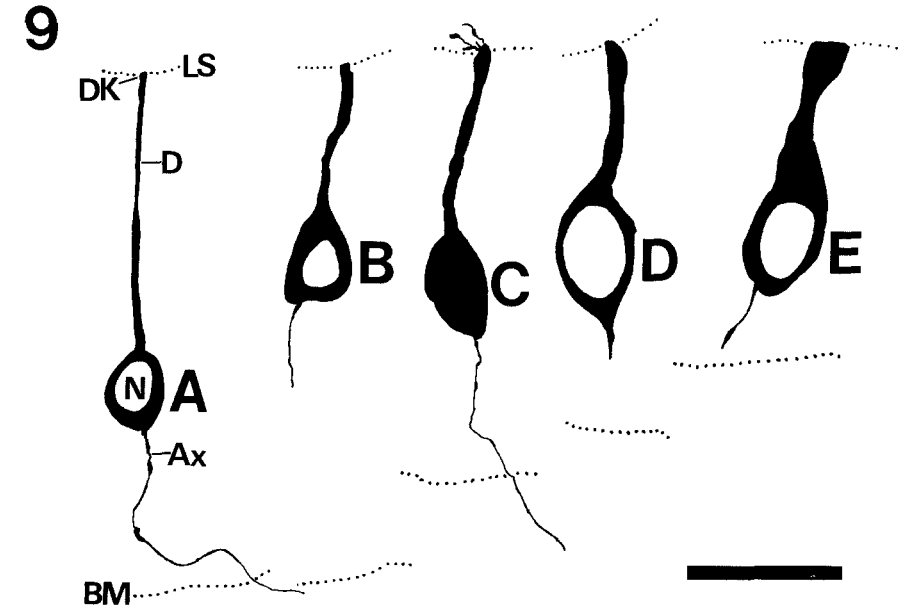

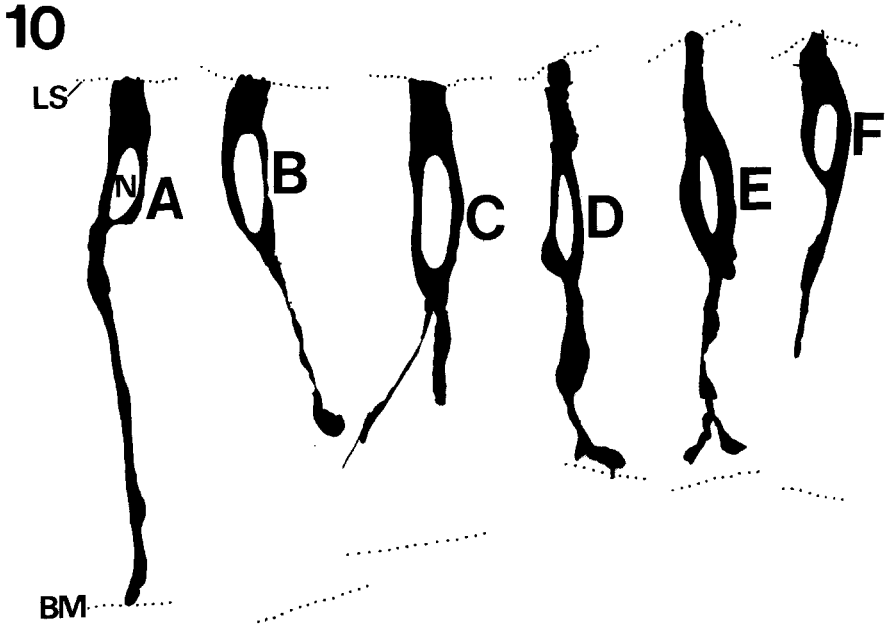

Fig. 9, 10. Camera lucida drawings from Golgi impregnated olfactory receptor neurons (**Fig. 9**) and sustentacular cells (**Fig. 10**). *N*, Nucleus. *Bar* 20 μm

Fig. 9. Representative olfactory receptor neurons arranged from the one with the smallest soma (*A*) to the largest (*E*). Each neuron sends a single dendrite (*D*) to the luminal surface (*LS*) and a single axon (*Ax*) toward the basement membrane (*BM*)

Fig. 10. Sustentacular cells can be divided into two classes; cells *A–C* have a broad supranuclear region reaching the luminal surface (*LS*), and cells *D–F* have a narrow or tapered supranuclear region. Some cells of each class have the infranuclear cytoplasm resting on the basement membrane (*BM*). Some cells have a single infranuclear cytoplasmic process (A, B, F), whereas others have a bifurcated one (C and E)

Fig. 5. Low-power scanning electron micrograph of the olfactory organ, ventral view. The olfactory organ is composed of two rows of lamellae (*L*) separated by a raphe (*R*). Each lamella has a free thickened edge of a tapered protruding process (*P*). *OB*, Olfactory bulb. *Bar* 500 μm

Fig. 6. Transverse paraplast section of the olfactory lamellae (*L*) present in the nasal cavity (*NC*), stained by the Klüver-Barrera method. The medial (*me*) is top and ventral (*ve*) is right. Each lamella is covered with an epithelium; folds (*arrows*) are seen in the epithelium except at the ventral ends. Cartilage (*C*) covers the olfactory organ and olfactory bulb (*OB*). *Bar* 500 μm

Fig. 7. Neuroepithelium covering each olfactory lamella, 1-μm-thick epoxy section stained with toluidine blue-O. The olfactory epithelium contains one row of nuclei of sustentacular cells (*NSC*) near the luminal surface, a few rows of nuclei of olfactory receptor neurons (*NOR*), and one row of nuclei of basal cells (*NBC*). One mitotic cell (*MC*) can be seen among the *NBC*. Olfactory nerve bundles (*ON*) are visible in the lamina propria. *PC*, Pigmented cell. *Bar* 50 μm

Fig. 8. Two neuroepithelia, facing each other via the nasal cavity. The free surface is mostly occupied by sustentacular cells (*SC*) with cilia (*ci*) at their apical ends. Bipolar olfactory receptor neurons (*ORN*) send dendrites (*D*) between the *SC* to the free surface. A mitotic cell (*MC*) is located among basal cells (*BC*). Note that the cilia from each epithelial surface are oriented in the same direction. *Bar* 10 μm

different cell types present in the OO of the clearnose skate by means of both light and electron microscopes as a background to embryological and experimental studies.

Materials and methods

Adult clearnose skates, *Raja eglanteria*, were captured passively off Sarasota, Florida, in nets. The adults were maintained in controlled-environment, recirculating sea water tanks, where breeding activity and subsequent egg-laying took place. Water temperature ranged from 20 to 22°C and salinity from 30 to 35 parts per thousand. Eggs were incubated under the same conditions. After the 11- to 13-week incubation period, offspring hatched and were reared on a diet of finely diced shrimp, squid, and herring or sardines. In relation to the laboratory conditions for the skates, we complied with the Principles of Laboratory Animal Care established by the National Institutes of Health (USA). Juvenile skates, 2–3 months after hatching (body weight 16–48 g), were used for this study. Before they were killed all the animals were deeply anesthetized with 0.1% MS-222 (tricaine-methane sulfonate, Sigma Co.) in filtered sea water. Five specimens were dissected for gross anatomy. For the light-microscope (LM) study, nasal regions of six animals were fixed by immersion in Bouin's fluid for at least 24 h, dehydrated through a graded ethanol series followed by methylsalicylate and toluene, and embedded in paraplast. Paraplast-embedded tissue blocks including the OO and OB were cut at 10 μm in transverse ($n=3$), sagittal ($n=2$), and horizontal ($n=1$) planes. Hematoxylin-eosin, Klüver-Barrera, and Alcian blue stains were used for the paraplast sections.

For Golgi and electron microscopic observations, skates were transcardially perfused with elasmobranch Ringer's, followed by a fixative (4% paraformaldehyde (PFA) plus 1% glutaraldehyde (GA) in 0.1 M phosphate buffer (PB)). The OO and OB were excised and immersed in 2% PFA plus 2.5% GA containing PB at 4°C overnight. For the rapid Golgi study, small pieces of the OO were processed as reported previously (Takami and Graziadei 1991), sections cut at 50 μm being routinely observed. For the transmission electron microscope (TEM) study ($n=5$), small pieces of the OO were postfixed with 1% buffered OsO_4 for 2 h, stained en bloc with 1.5% aqueous solution of uranyl acetate for 40 min, and processed as described previously (Takami and Hirosawa 1990). A substitute of Epon 812, LX-112 (Ladd Res.) was used for embedding. A Jeol-1200EX TEM was used at an accelerating voltage of 80 kV. For scanning electron microscope (SEM) study ($n=5$), the OO was dissected into small tissue blocks in PB after overnight fixation of PFA and GA. The mucous layer covering the epithelia was removed by gentle shaking of the tissue blocks in PB followed by 5% GA in PB for 2 h. Before postfixation with OsO_4 for 2 h, some parts of the organ were reduced to small pieces to expose the lateral surface of the lamellae. Pieces were then stained with 1% tannic acid or 1.5% uranyl acetate for 1 h, dehydrated with a graded series of ethanols to absolute ethanol, transferred into a critical point dryer (Baltzers, Switzerland), and critical pointdried with liquid CO_2. After sputter coating with gold-palladium, the tissue blocks were observed under a JEM-840 (Jeol, Japan) operated at 10 or 15 kV with variable working distances (6–46 mm).

Results

The two openings of each OO in this species are located on the ventral surface of the body (Fig. 1). The openings are incompletely subdivided into an anterior incurrent nostril and a posterior excurrent nostril (Fig. 2). The incurrent nostril is ovoid, and its walls project inward to continue in the nasal cavity. The excurrent nostril is oval,

Fig. 11–16. Transmission electron micrographs of type 1 receptor neurons

Fig. 11. Low-power image of the olfactory epithelium showing three type 1 receptor neurons (*OR*1). Their dendrites (*D*) are seen among sustentacular cells (*SC*). Lamellae of endoplasmic reticulum (*ER*), lysosomes (*Ly*) and mitochondria (*m*) can be seen in the *OR*1. *Arrow* indicates a pair of centrioles whose higher magnification is shown in Fig. 14. Accumulation of mitochondria (*m*) is present in the apical region of *SC*. On the epithelial surface, a cross-sectioned type 2 neuron (*OR*2) is also seen. Nuclei (*nl*) of *OR*1 and *SC* are indicated. *Bar* 5 μm

Fig. 12. Apical region of a dendrite and its ending, dendritic knob (*DK*), of a type 1 neuron. Many mitochondria (*m*) can be seen below the *DK*. Many vesicles (*v*) and some microtubules (*t*) are present in the dendrite as well as the *DK*. Junctional complexes (*jc*) are visible between the dendrite and adjacent sustentacular cells (*SC*). *Bar* 1 μm

Fig. 13. Dendritic knob with microvilli (*mv*). The arrangement of microtubules (*t*) becomes random near the knob. Cores of filaments (*arrowheads*) are prominent in the *DK*. Smooth vesicles (*v*) and filaments (*f*) continuous to the inside of microvilli (*mv*) can also be seen. *ci*, Cilium of a sustentacular cell. *Bar* 0.5 μm

Fig. 14. High-power image of a pair of centrioles (*c*) close to microtubules (*t*) in the dendrite in Fig. 11. *Bar* 0.5 μm

Fig. 15. Supranuclear region of a *OR*1 neuron showing Golgi complex (*G*) and mitochondria (*m*). *Bar* 1 μm

Fig. 16. Well-developed lamellae of rough endoplasmic reticulum (*rER*) in a type 1 receptor neuron. The lamellae of the *rER* occupy the cytoplasm between the nucleus (*N*) and the cell membrane (indicated by *arrowheads*) adjacent to a sustentacular cell (*SC*). *Bar* 1 μm

Fig. 17–20. Transmission electron micrographs showing type 2 receptor neurons

Fig. 17. Dendrite (*D*) and dendritic knob (*DK*) of a type 2 receptor neuron and adjacent sustentacular cells. Short and thick microvilli, "stiff microvilli" (*smv*), project from the *DK*. A bundle of filaments (*bf*) in each microvillus can be traced down within the *D* about 9 μm from the base of the *smv*. Well-developed Golgi complexes (*G*) are present in the region above the nuclei of the sustentacular cells (*NSC*). *Bar* 2 μm

Fig. 18. Higher magnification of the dendritic knob shown in Fig. 17. This knob contains three bundles of filaments (*bf*), each projecting into a stiff microvillus (*smv*). Numerous smooth vesicles (*v*) and a coated vesicle (*cv*) can be seen between each pair of *bf* and in the peripheral cytoplasm. Mitochondria (*m*) are also visible in the *DK*. The junctional complex (*arrows*) can be seen between adjacent sustentacular cells. *Bar* 1 μm

Fig. 19. Cross-section of "stiff microvilli" (*smv*), logitudinal section of a microvillus (*mv*) of a type 1 receptor neuron, and a cilium (*ci*) of a sustentacular cell. The *smv* have glycocalyx (*arrows*) in the outer surface of the membrane and cross-sectioned filaments (*arrowheads*) in their cytolasm. *Bar* 0.5 μm

Fig. 20. Longitudinal section including soma and dendritic knob (*DK*) of a type 2 receptor neuron (*OR*2). To the left of this cell lies the soma of a type 1 receptor neuron (*OR*1). The higher magnification of the supranuclear region of the *OR*2 is shown in Fig. 21. The nucleus of this *OR*2 is at the same level as a nucleus of a sustentacular cell (*NSC*). Secretory granules (*sg*) of a goblet cell are also visible. Lipofuscin granules (*Li*) are seen in the supranuclear region of a sustentacular cell. *nl*, Nucleolus. *Bar* 5 μm

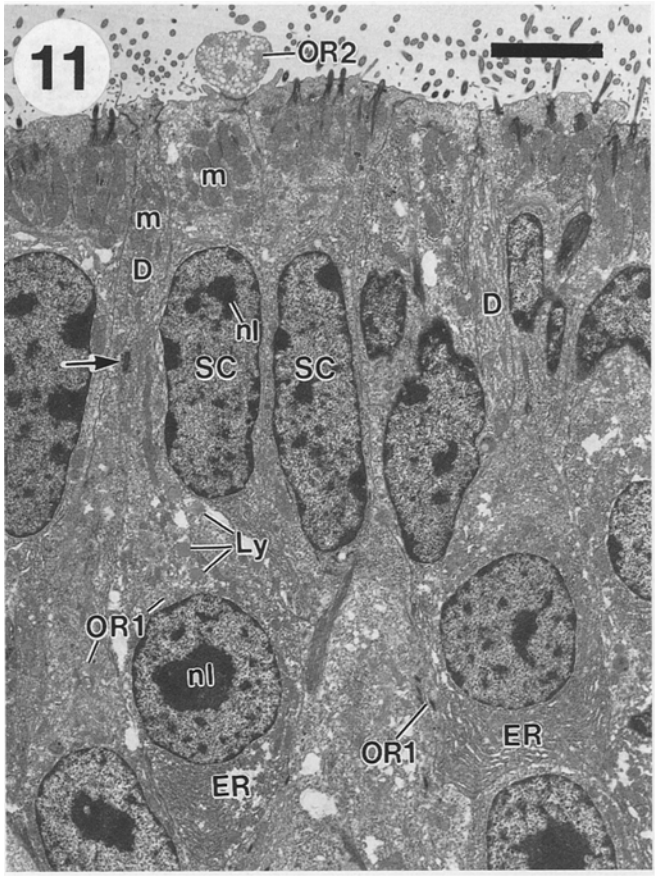
11
OR2
m
m
D
nl
SC
SC
D
Ly
OR1
nl
ER
OR1
ER

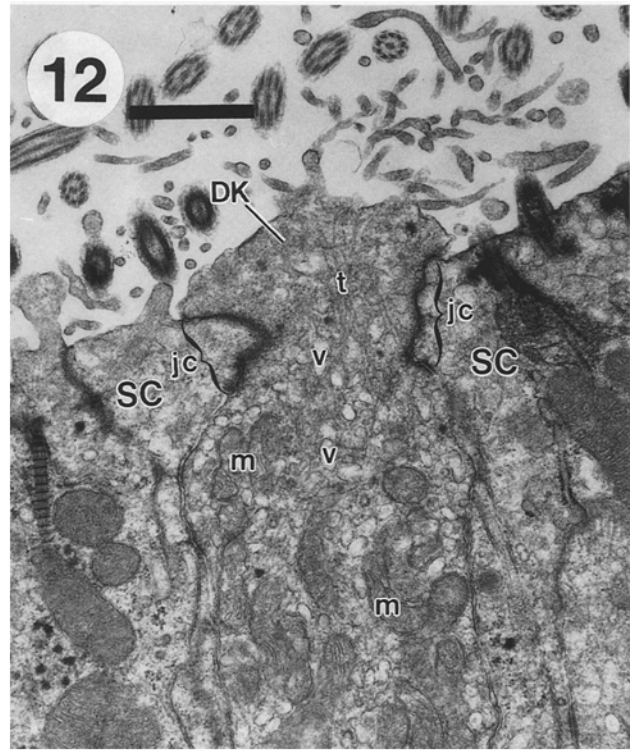
12
DK
t
jc
jc
v
SC
SC
m
v
m

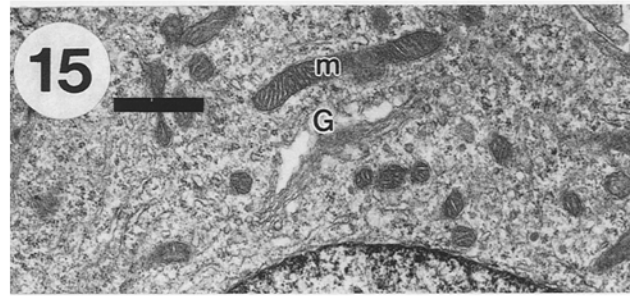
15
m
G

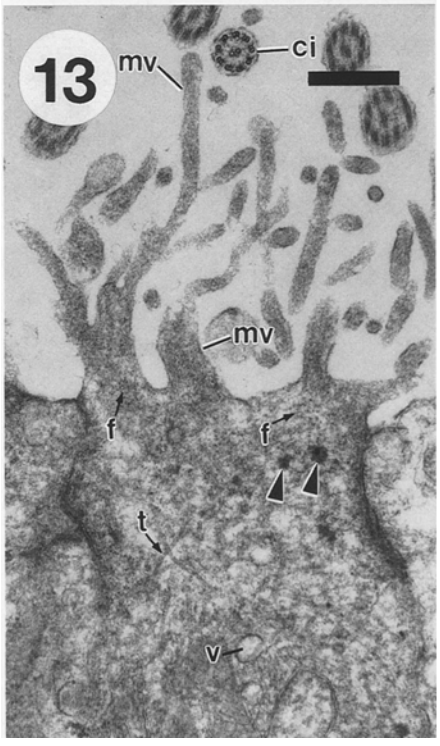
13
mv
ci
mv
f
f
t
v

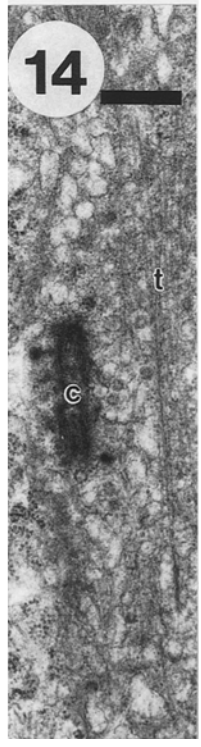
14
t
c

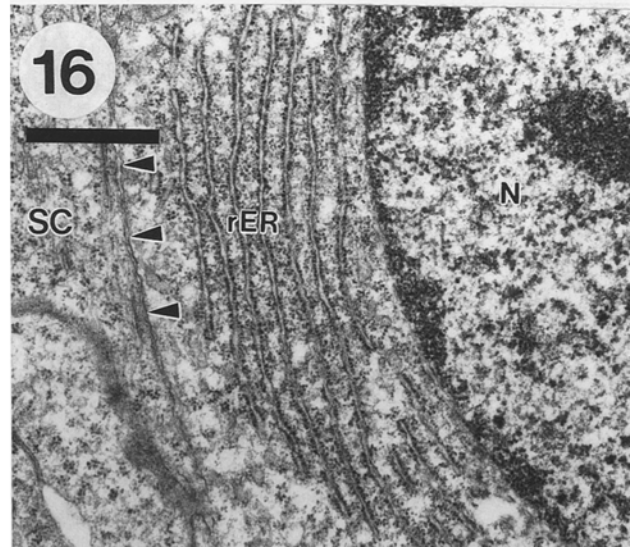
16
SC
rER
N

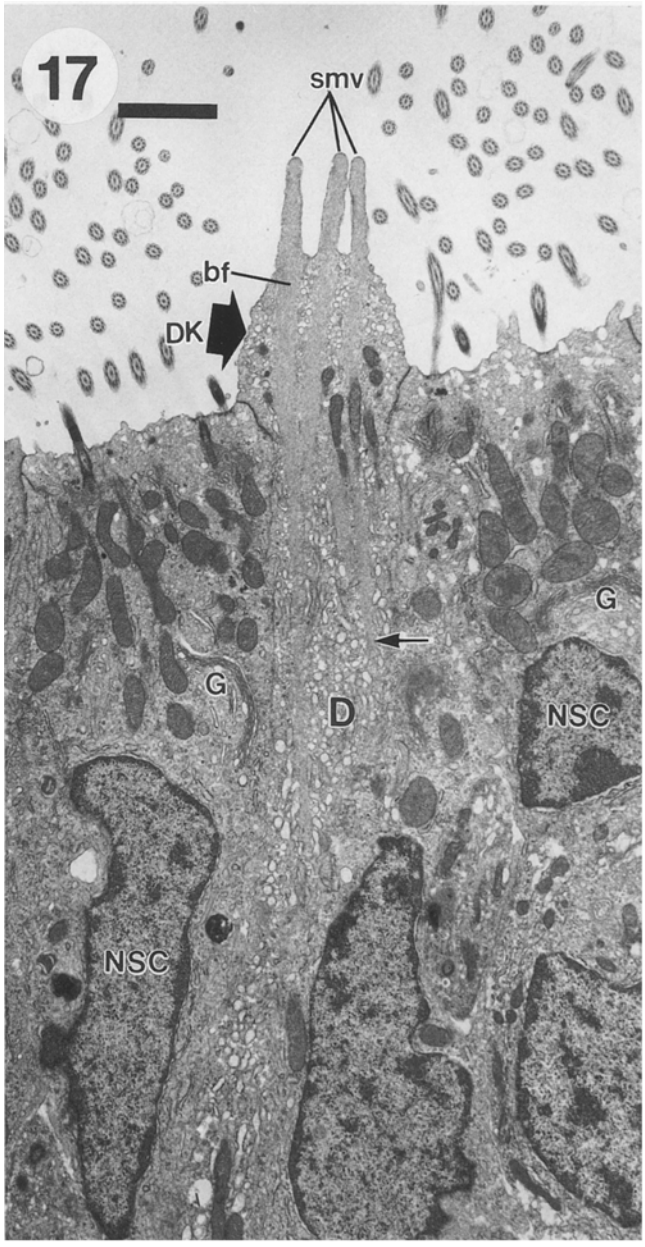
17
smv
bf
DK
G
G
D
NSC
NSC

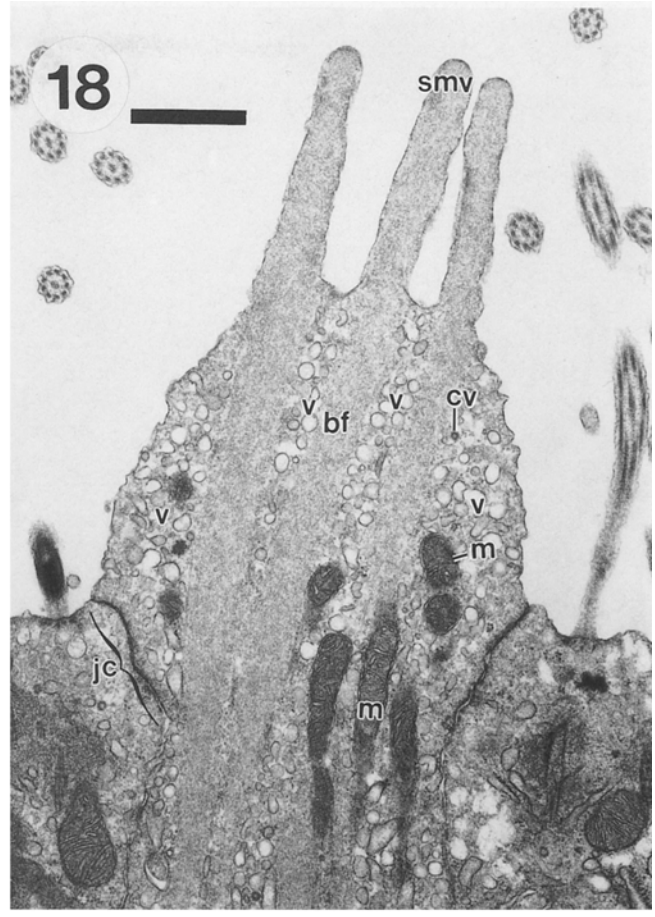
18
smv
v
bf
v
cv
v
v
m
jc
m

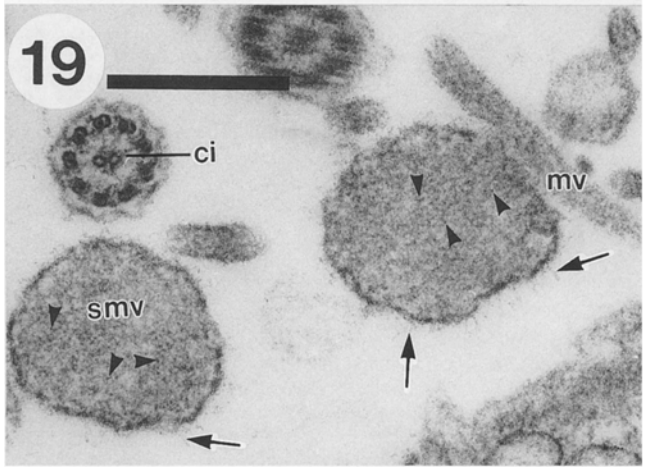
19
ci
mv
smv

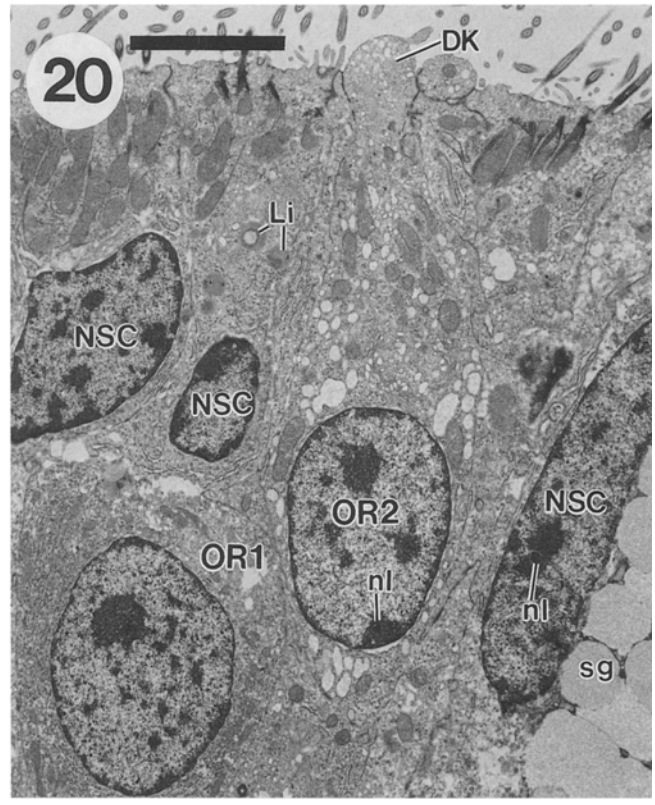
20
DK
Li
NSC
NSC
OR2
NSC
OR1
nl
nl
sg

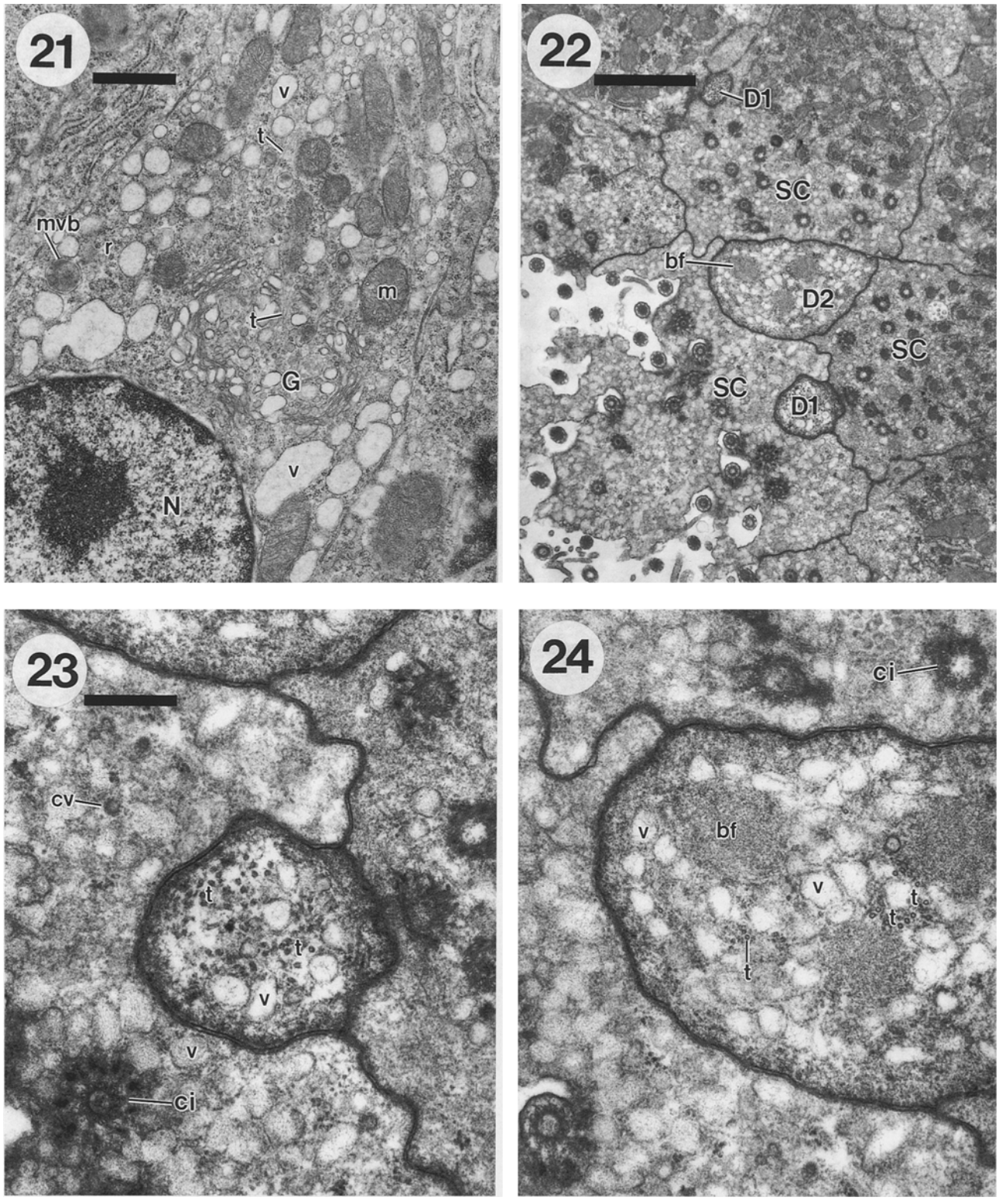

Fig. 21. Higher-power image of the nucleus and supranuclear region of the type 2 receptor neuron seen in Fig. 20. Above the nucleus (*N*), a well developed Golgi complex (*G*) is present. Numerous vesicles (*v*) of various sizes, many mitochondria (*m*), clusters of free ribosomes (*r*), and a multivesicular body (*mvb*) can be seen. Microtubules (*t*) are present within and above the *G*. *Bar* 1 μm

Fig. 22. Cross-sectioned apical region of the olfactory epithelium at low magnification. Two dendrites of type 1 neurons (*D*1), and one of type 2 (*D*2) with three bundles of filaments (*bf*) are completely surrounded by sustentacular cells (*SC*). Higher magnification of dendrites *D*1 and *D*2 is shown in Figs. 23 and 24, respectively. *Bar* 2 μm

Fig. 23. Higher magnification of one of the type 1 dendrites in Fig. 22. Microtubules (*t*) and vesicles (*v*) can be seen in its cytoplasm. In the cytoplasm of the adjacent sustentacular cell, numerous vesicles (*v*), a coated vesicle (*cv*), and a cross-sectioned basal body of a cilium (*ci*) are present. *Bar* 0.5 μm

Fig. 24. Higher magnification of the type 2 dendrite in Fig. 22. Among three bundles of filaments (*bf*), numerous vesicles (*v*) and microtubules (*arrowheads*) can be seen in a small group. Magnification as in Fig. 23

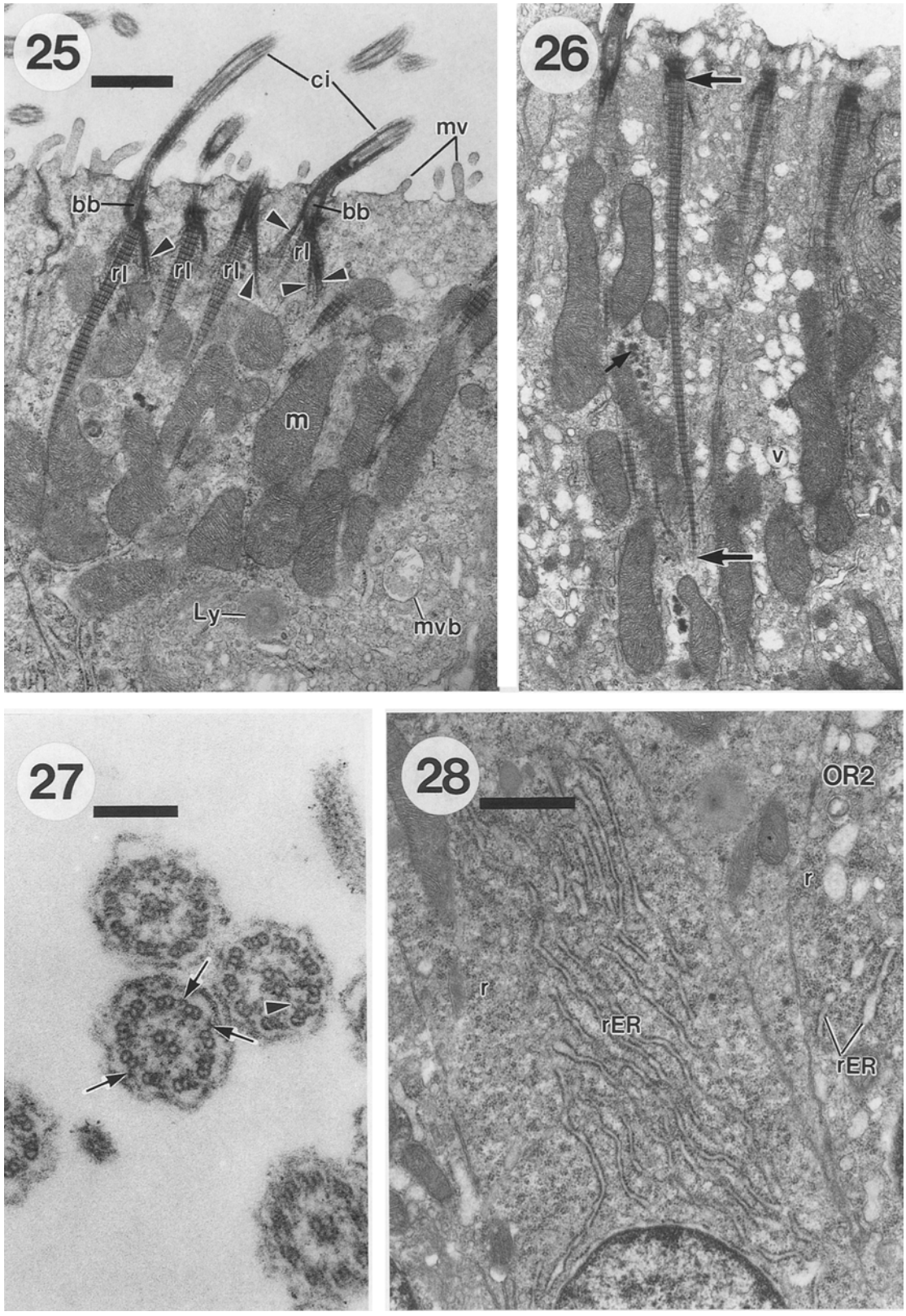

Fig. 25–28. Transmission electron micrographs of sustentacular cells and a type 2 receptor neuron

Fig. 25. Apical part of a sustentucular cells above the Golgi area. The apical membrane of the cell is covered with many cilia (*ci*) and short microvilli (*mv*). The basal parts of the cilia are continuous with basal bodies (*bb*) and rootlets (*rl*). Subrootlets (*arrowheads*) are associated with *rl*. Accumulation of mitochondria (*m*), a multivesicular body (*mvb*) and a lysosome (*Ly*) can also be seen. *Bar* 1 μm

Fig. 26. Example of a long rootlet (*rl*). Its length (between the two *larger arrows*) is about 7 μm. Electron-dense bodies (*small arrow*) are present among numerous vesicles (*v*) and rootlets. The magnification is the same as in Fig. 25

Fig. 27. High magnification of cross-sectioned cilia of sustentacular cells. A 9+2 arrangement of microtubules, dynein armes (*arrows*), and a radial spoke (*arrowhead*) can be seen. *Bar* 0.2 μm

Fig. 28. Supranuclear part of a sustentacular cell showing well-developed rough endoplasmic reticulum (*rER*) and free ribosomes (*r*). An adjacent type 2 receptor neuron (*OR2*) contains a few single lamellae of *rER* and clusters of free ribosomes. *Bar* 1 μm

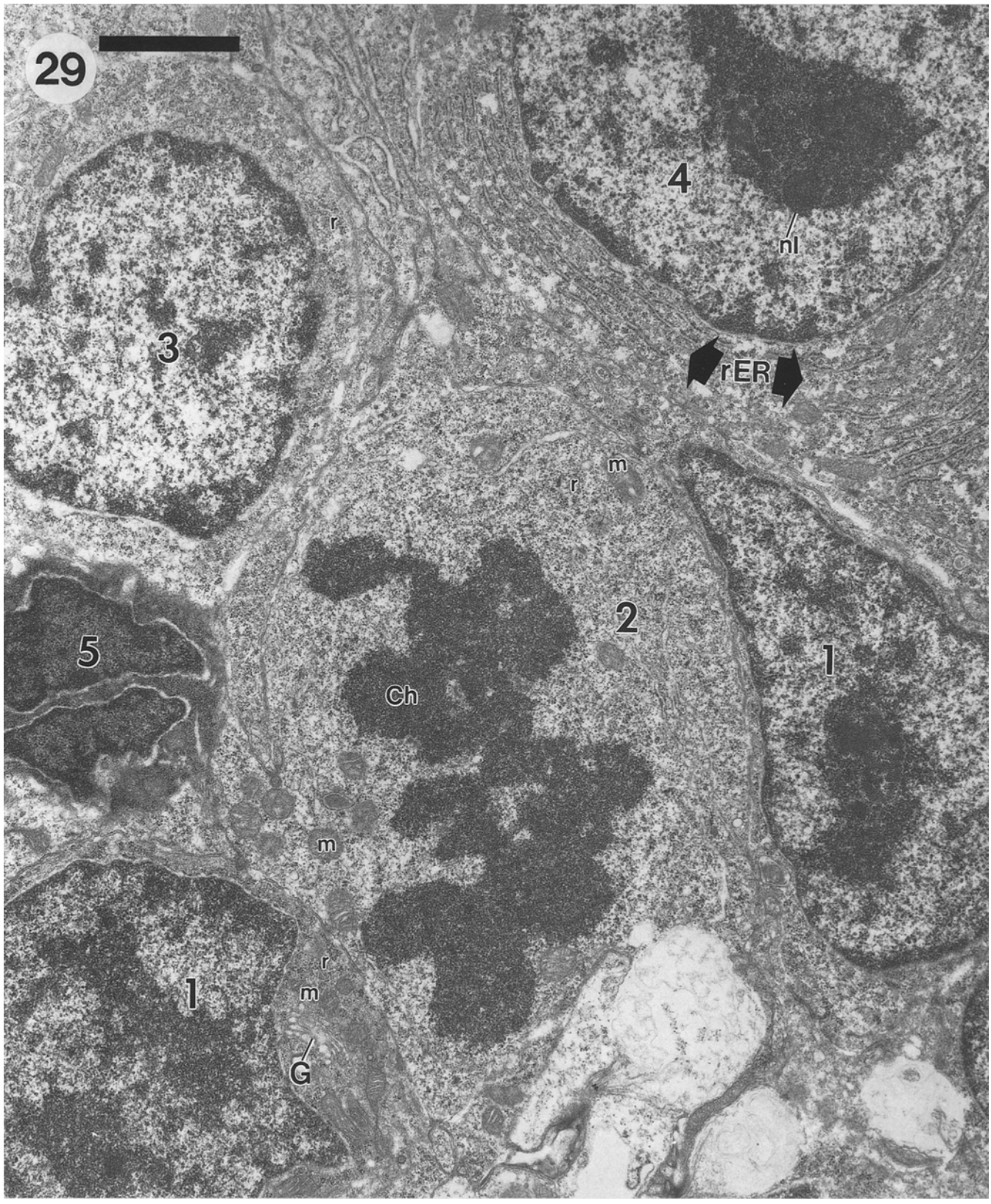

Fig. 29. Basal region of the neuroepithelium showing several types of cells. Basal cells (1) have nuclei of irregular shape, and their cytoplasm contains the Golgi complex (*G*), small mitochondria (*m*), and clusters of free ribosomes (*r*). Chromosomes (*Ch*), ovoid mitochondria, and clusters of free ribosomes are seen in a mitotic cell (2). A putative differentiating cell (3) contains a large number of free ribosomes. A putative mature receptor neuron (4) has a prominent nucleolus (*nl*) in the nucleus and *rER*. A cell with electron-dense cytoplasm and nucleus (5) can also be seen. *Bar* 2 μm

with a thin valvular extension along its outer margin. A tapering nasal flap arises from the anterior margin of these nostrils. The two nostrils are connected into the OO at its ventrolateral margin (Fig. 3). Each OO has an ellipsoid shape (Figs. 3, 4), the convex aspect of which is oriented dorsally (Fig. 4). The nasal cavity is located in the concave surface of the OO (Fig. 3). The convex surface of the OO is pigmented. A tubular OB extends from the lateral to the medial edge of the convex (dorsal) surface of the OO (Fig. 4).

Each OO is composed of two rows of lamellae, some 20 per organ, separated by a transverse raphe (Fig. 5). The lamellae are larger in the middle of the organ and decrease in size toward the lateral and medial ends. Opposite the raphe, each lamella has a free thickened edge or a tapered protruding process.

A transversely cut paraplast section through the middle of the OO is shown in Fig. 6. The lamellae are covered with the sensory epithelium, which shows folds that disappear toward their ventral free margin. An epoxy section (Fig. 7) shows a part of these folds. The sensory epithelium is pseudostratified, 70 to 80 μm thick, and prominent nerve bundles are present in the lamina propria. Oblong nuclei located close to the luminal surface (in the upper quater of the epithelium) belong to sustentacular cells. Two or three layers of lightly stained, round nuclei with clearly defined nucleoli, which are located below the sustentacular cell nuclei, belong to the receptor neurons. Basal cells can be seen at the base of the sensory epithelium, where mitotic figures are commonly found. Glands were not observed in the lamina propria of the sensory epithelium. Cell shape and morphology of the epithelial components can be demonstrated more clearly at higher magnification (Fig. 8). The sustentacular cells have cilia regularly oriented at their luminal surface. A darkly stained band zone observed at the base of the cilia can be identified by TEM as a regular row of basal bodies (see below). The soma of the receptor neurons has a flask-like shape and continues apically in a process, the dendrite, that reaches the free surface. The basal cells, in immediate contact with the basement membrance, have an irregular nucleus and globose cytoplasm.

The rapid Golgi method demonstrates clearly the total profile of both receptor neurons and sustentacular cells. Representative examples of receptor neurons are shown in Fig. 9; cell A has the smallest soma, and cell E the largest. The apical pole of the soma in these neurons continues in a single dendrite that reaches the lumen and ends in a dendritic knob. At the proximal pole of the soma originates a fine, unbranched axon. There is great variation in the size of the somata and in the length of the dendrites depending on the position of the soma in the epithelium. Cells with larger somata (D, E) also have thicker dendrites. In sustentacular cells (Fig. 10), the infranuclear cytoplasm tapers into at least two morphological types, one with a nearly rectangular cytoplasm (A–C) and the other with a tapering supranuclear cytoplasm (D–F). In both types, the foot process reaching the basement membrane can have different configurations. The foot process of cell A, for example, reaches the basement membrane, whereas the cytoplasm of cell B forms a bulbar process ending in the lower two-fifths of the OE. The infranuclear part of cell C has a thin process originating from a main process, and neither reaches the basal region of the epithelium. Cell D is another example of a cell spanning the entire epithelium with a foot process attached to the basement membrane. Cells E and F are other examples of the diverse dispositions of the infranuclear cytoplasm.

TEM observations clearly demonstrate that two types of olfactory receptor neurons can be recognized in the skate. The first type, designated as type 1, posesses numerous, long, slender microvilli, whereas in type 2 the microvilli are fewer, shorter, and thicker. These distinguishing characteristics could not have been identified with the Golgi method alone.

The type 1 cell is a commonly described receptor neuron, already observed in other species of selachians (see Discussion). Three type 1 receptor neurons are illustrated in Fig. 11, which shows the round nuclei with prominent nucleoli that are characteristic of all the neurons in these animals. The dendrites, surrounded by the cytoplasm of sustentacular cells, which are recognized by their characteristic oblong or oval nuclei, reach the free surface of the epithelium, where they terminate in typical dendritic knobs (Figs. 11–13). Some dendritic knobs appear as small swellings (Fig. 12). As a rule, the apical part of these dendrites is complicated by the presence of microvilli, which have a thicker proximal diameter (some 300 nm) tapering in the distal region to about 90 nm (Fig. 13). The apical region of the dendrites is usually filled with mitochondria, although the terminal knob is devoid of these organelles (Fig. 12). Numerous smooth vesicles are present among these mitochondria, as well as within the dendritic knobs (Figs. 12, 13). Microtubules are observed in the cytoplasm of dendrites (Fig. 14), and they end just

Fig. 30–33. Photographs of mucous cells

Fig. 30. Alcian blue-stained paraplast section from the peripheral part of the olfactory organ where no olfactory epithelium is present. Many Alcian blue-positive goblet cells (*arrows*) and cells with Alcian blue-negative cytoplasm (*arrowheads*), "light cells", and extensively pigmented connective tissue (*CT*) can be seen. *Bar* 100 μm

Fig. 31. Alcian blue-stained paraplast section including the dorsal edges (at the left) of three lamellae. Goblet cells (*arrows*) and "light cells" (*arrowheads*) are seen in the dorsal edges of all these lamellae; single goblet cells are seen in the olfactory epithelium (*OE*) . *Bar* 100 μm

Fig. 32. Alcian blue-stained paraplast section including the ventral ends of lamellae at the *right*. Each lamella contains the olfactory epithelium (*OE*) and non-sensory epithelium (*NE*), with goblet cells (*arrows*) and other cells, including "light cells" (*arrowheads*). Goblet cells and "light cells" are also seen in the *OE*. A mucus layer (*double arrowheads*) covering the surface of the *OE* can also be seen. *Bar* 100 μm

Fig. 33. Toluidine blue-stained epoxy section from the peripheral part of the olfactory organ. Many goblet cells with secretory granules (*sg*) occupy the luminal surface. Their nuclei (*N*) are localized at the base of the cytoplasm. The cell indicated by an *open arrow* has a light infranuclear cytoplasm, but the supranuclear cytoplasm is not a light as that of a "light cell" (*arrowhead*). Aggregates of dark nuclei (*) are seen below the layer of goblet cells. *Bar* 50 μm

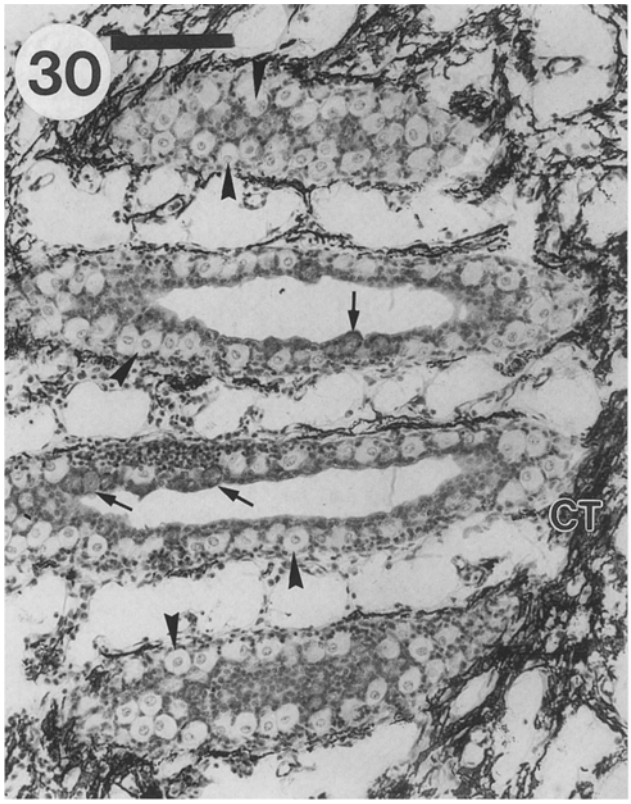
30
CT

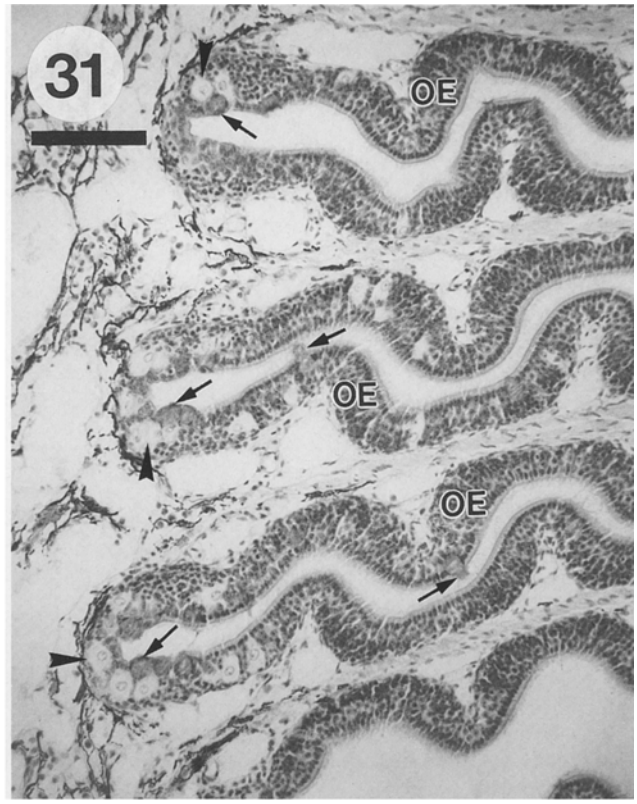
31
OE
OE
OE

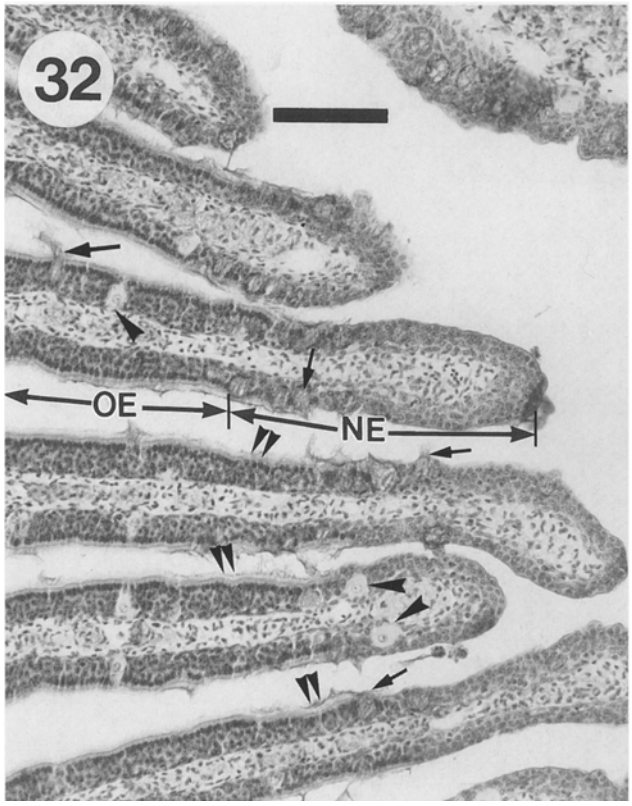
32
OE
NE

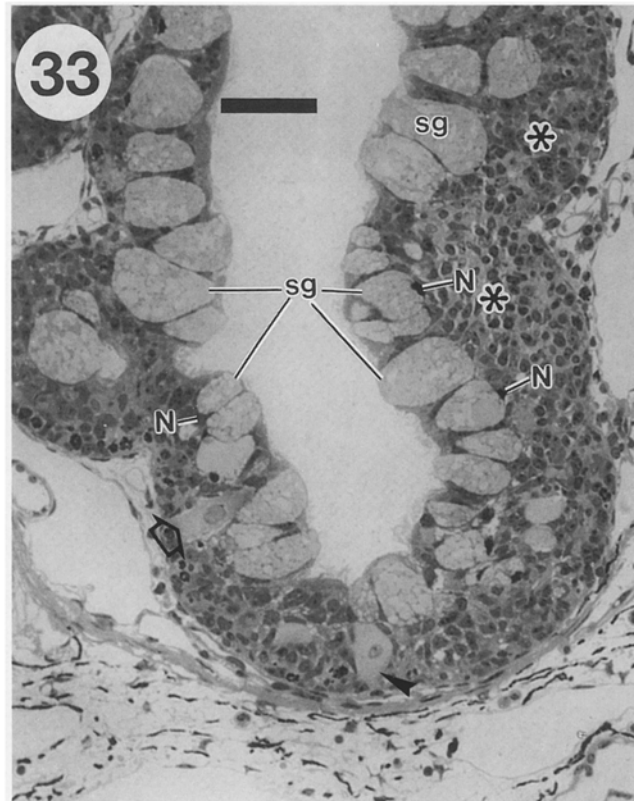
33
sg
sg
N
N
N

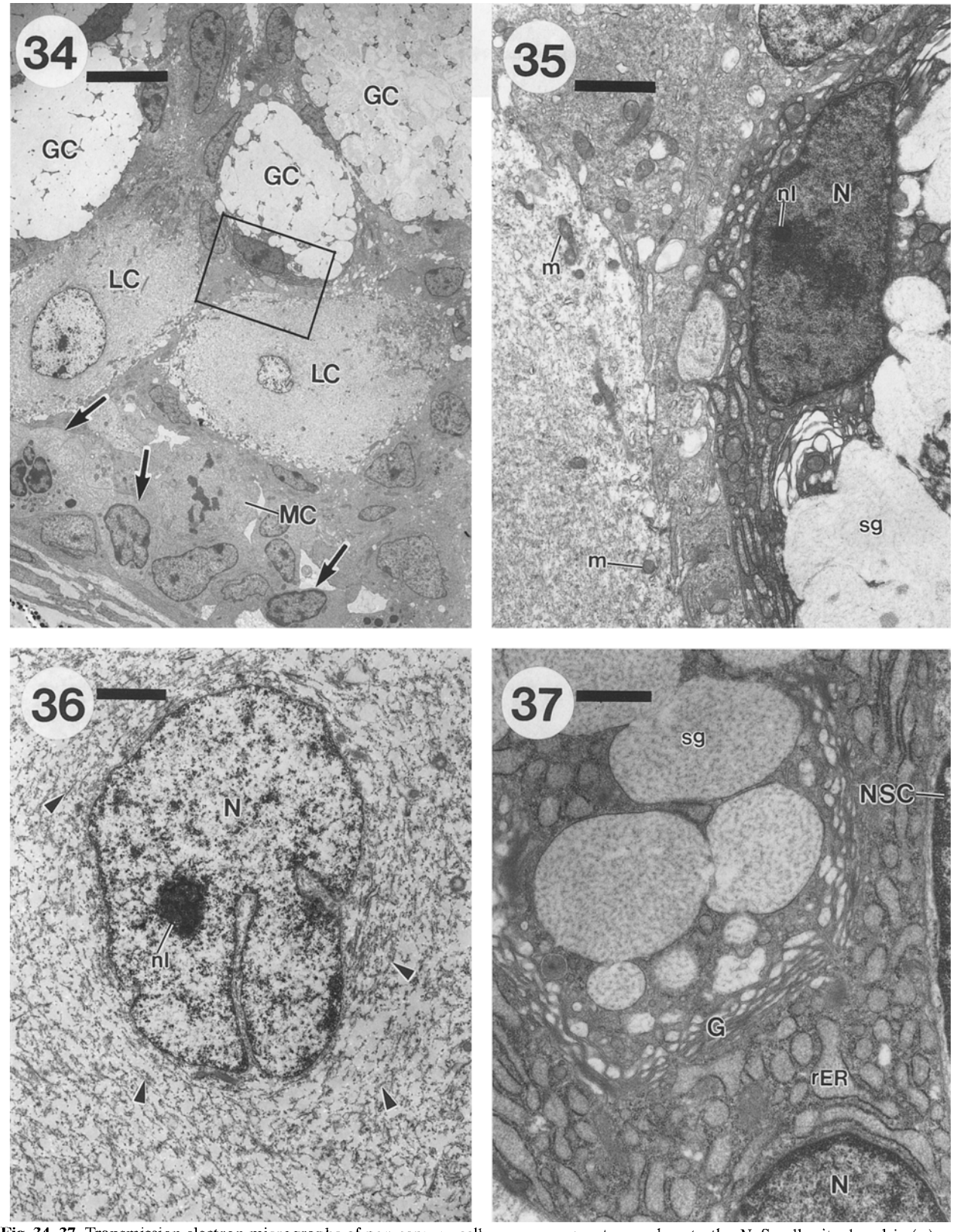

Fig. 34–37. Transmission electron micrographs of non-sensory cells

Fig. 34. Thin section close to the one of Fig. 33. The electron density of secretory granules of goblet cells (*GC*) is variable. No granules are present in "light cells" (*LC*). The *boxed area* is shown at higher magnification in **Fig. 35**. A mitotic cell (*MC*) is seen near the base of this epithelium. Some small cells (*arrows*) can be interpreted as immune system cells. *Bar* 10 μm

Fig. 35. Basal region of a goblet cell (at right) and an adjacent "light cell"; see **Fig. 33**. Nucleus (*N*) of the goblet cell is rich in heterochromatin and has a prominent nucleolus (*nl*). Secretory granules (*sg*) are present very close to the *N*. Small mitochondria (*m*) are seen in the fibrillar cytoplasm of the "light cell". *Bar* 2 μm

Fig. 36. "Light cell" with a lobulated nucleus (*N*) and a nucleolus (*nl*). Numerous fibrous elements (*arrowheads*) are seen in the cytoplasm. *Bar* 2 μm

Fig. 37. Supranuclear region of a goblet cell found in the olfactory epithelium. Numerous dilated cisternae of *rER* are present just above the nucleus (*N*). Above these are a well-developed Golgi complex (*G*) and secretory granules (*sg*). The nucleus of a sustentacular cell (*NSC*) can be seen at the right. *Bar* 1 μm

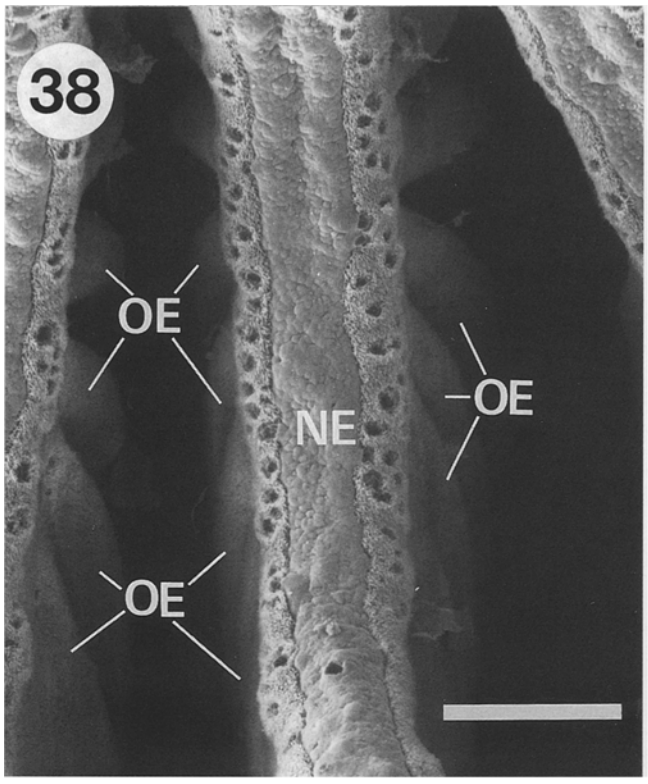
38
OE
NE
OE
OE

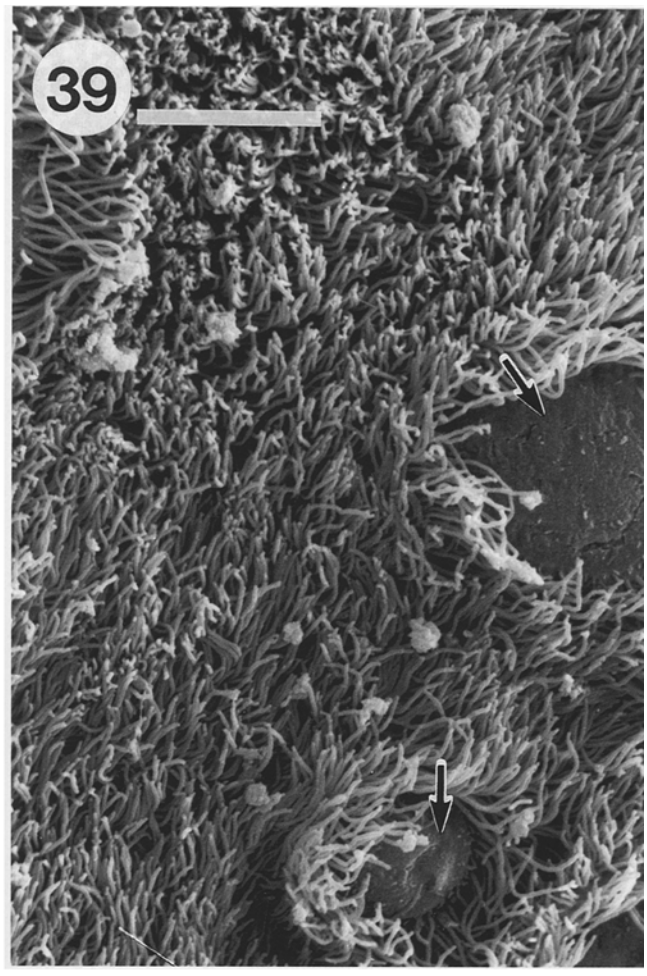
39

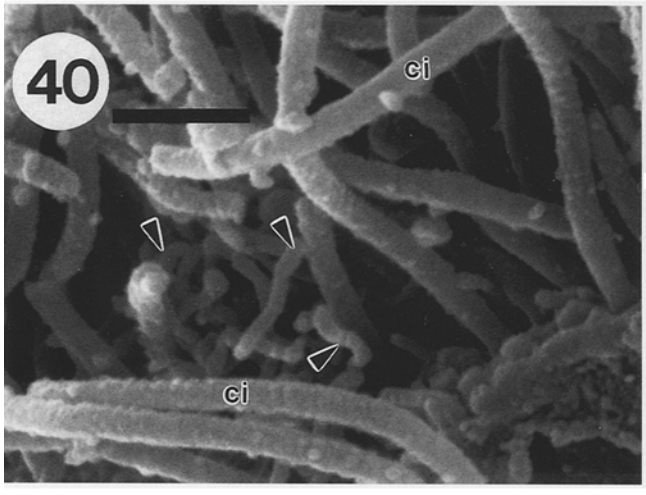
40
ci
ci

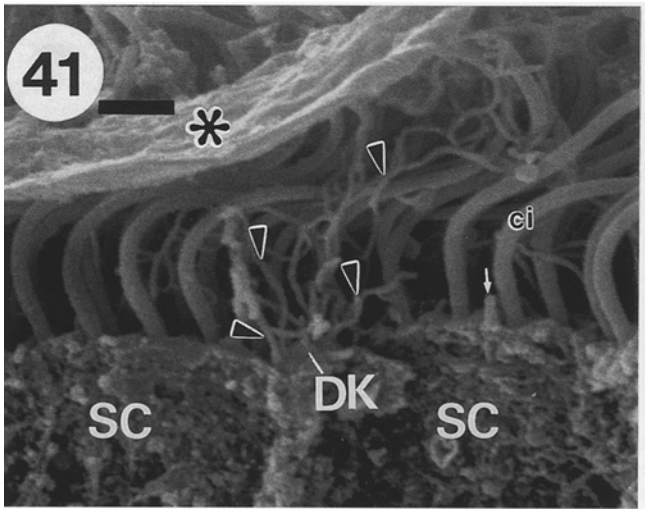
41
*
ci
DK
SC
SC

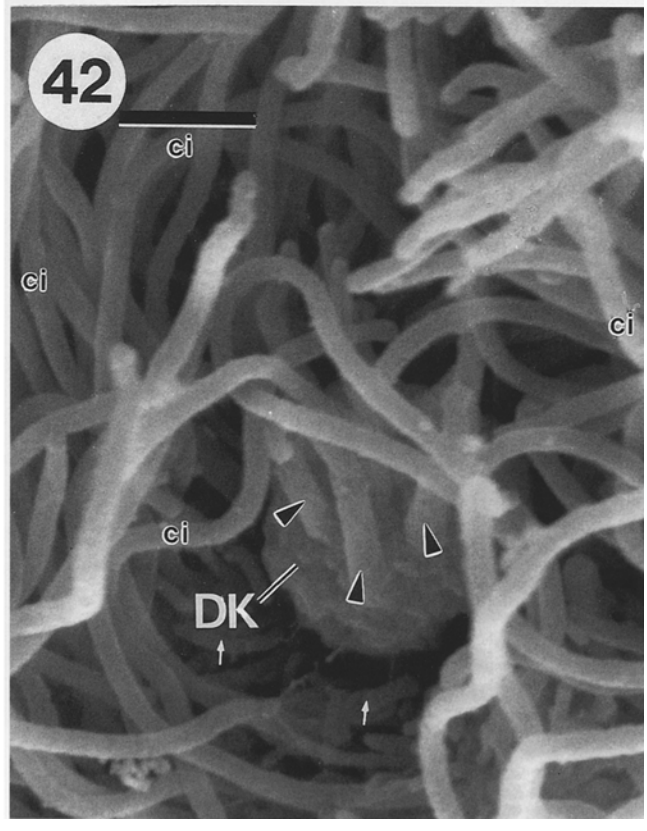
42
ci
ci
ci
ci
DK

at the base of the microvilli (Fig. 13). Aggregates of filaments also occur in the knob (Fig. 13). No cilia have been observed in these receptor neurons, but the presence of centrioles is not uncommon (Fig. 14). A Golgi complex is located in the supranuclear region (Fig. 15), but a characteristic organelle of these receptors is a well-developed system of cisternae of the rough endoplasmic reticulum (rER) (Figs. 11, 16).

The type 2 receptor neuron has a bulbar dendritic knob projecting distinctly into the lumen (Figs. 17, 18). A few small but thick microvilli originate from the knob, and each microvillus is filled with a tight bundle of filaments. The bundle runs from the distal tip of the microvillus down into the cytoplasm of the dendrite up to 5–9 μm from its base (Figs. 17, 18). Because each microvillus of the type 2 receptors is straight and is supported by a dense fibrillar core of filaments, these microvilli are termed *stiff microvilli*. The dendritic knob of these type 2 receptors contains numerous smooth vesicles (Fig. 18) together with a small accumulation of mitochondria (Figs. 17, 18). A cross-section of these microvilli is shown in Fig. 19. The diameter of the *stiff microvilli* (300–600 nm) is usually larger than that the diameter of the cilia in the sustentacular cells. The diameter of the filaments in the core of the microvilli was estimated to be 5 nm. A section of the base of the dendrite of a type 2 cell close to the perinuclear region is shown in Fig. 20. A considerable quantity of smooth vesicles is observed there, as well as in the infranuclear region. A higher-power electron micrograph of the supranuclear region is shown in Fig. 21, where a well-developed Golgi complex is shown as a characteristic feature of these neurons. The smooth vesicles associated with the Golgi complex are larger than those described previously in the dendrite. Numerous free ribosomes (polysomes) and a few microtubules are scattered in the cytoplasm among the Golgi profiles (Fig. 21). Characteristic stacks of rER profiles in these receptors were never observed (Fig. 28). The above characteristic organelles were used, with the details of their free dendritic endings, to distinguish type 2 from type 1 neurons.

Neither type of neuron seems to have a specific location in the sensory epithelium, and the two are often in close proximity (Figs. 11, 20). Preliminary observations have shown that type 1 neurons are more frequent than type 2, but the ratio and distribution pattern of these neurons were not quantified. A cross-section of the apical region of the OE shown in Fig. 22 demonstrates that both type 1 and type 2 neurons can be closely associated with sustentacular cells. As a rule, the dendrites of type 1 neurons are smaller in diameter (0.5 to 1.5 μm) than those of type 2 neurons (2.5 to 3.5 μm). Cross-sectioned microtubules and smooth vesicles, up to 40 microtubules per section (Fig. 23), are often observed in type 1 neurons. In the cross-section of a type 2 dendrite, three to seven round aggregates of filaments were observed, each representing the cross-section of a bundle filling the microvilli. Between the aggregates of filaments, smooth vesicles and some microtubules are present (Fig. 24). The density of microtubles in type 2 neurons is noticeably less than that in type 1.

The heteromorphic character of the sustentacular cells is restricted to the soma shape (Fig. 10); their free lumen surface was consistently provided with both cilia (Figs. 11, 12, 17–20, 25, 27) and short microvilli (Figs. 12, 17, 25). A large accumulation of mitochondria is a common feature of their apical cytoplasm (Figs. 11, 17, 20, 25, 26) and lends the overall appearance of a dense region in LM sections (Figs. 7, 8). The cilia in the sustentacular cells have long rootlets (Figs. 25, 26) extending some 5 μm into the apical cytoplasm among the numerous mitochondria (Fig. 26). The main rootlet of each cilium branches often in a subrootlet system (Fig. 25). Each cilium has a 9 + 2 arrangement of tubules (Figs. 19, 27), and at high magnification dynein arms can be demonstrated (Fig. 27). A well-developed Golgi complex is typical of

Fig. 38–42. Scanning electron micrographs

Fig. 38. Ventral view of the olfactory lamellae. The ventral surface of the lamellae is covered by a non-sensory epithelium (*NE*); secondary folds on the side of the lamellae are covered with the olfactory epithelium (*OE*). *Bar* 500 μm

Fig. 39. Surface view of a part of a fold covered with olfactory epithelium. Apical poles of two goblet cells (*arrows*) can be seen among a plexus of cilia and microvilli. *Bar* 5 μm

Fig. 40. High magnification of the surface of the olfactory epithelium. Microvilli (*arrows*) of type 1 receptor neurons are seen among cilia (*ci*) of sustentacular cells. *Bar* 1 μm

Fig. 41. Lateral surface of the apical region of the olfactory epithelium. A dendritic knob (*DK*) of a type 1 receptor neuron is shown between two sustentacular cells (*SC*) with cilia (*ci*). Microvilli (*arrowheads*) originating from the *DK* form the complex meshwork. A strand of a putative mucus (*) remains to cover the surface. The *small arrow* indicates a sustentacular cell's microvillus. *Bar* 1 μm

Fig. 42. Dendritic knob (*DK*) of type 2 neuron. *Stiff microvilli* (*arrowheads*) projecting from the *DK*are thicker than cilia (*ci*) of sustentacular cells. *Small arrows* indicate microvilli of the sustentacular cells. *Bar* 1 μm

Fig. 43–46. Scanning electron micrographs

Fig. 43. Lateral view of the fractured olfactory epithelium. Olfactory receptor neurons (*ORN*) with dendrites (*D*) and axons (*Ax*), and surface of sustentacular cells (*SC*) are seen sideways. Foot-like processes (*) of the *SC* can also be seen. *Bar* 5 μm

Fig. 44. Surface view of the non-sensory epithelium (*NE*). Cells located in the center have short microvilli on their apical surfaces, and the cell boundaries are clearly seen. This epithelium changes to ciliated epithelium on both sides, where hole-like structures (*arrows*) are seen. The *boxed area* is shown at higher magnification in Fig. 45. *Bar* 20 μm

Fig. 45. Enlargement of the boxed area in Fig. 44 (rotated nearly 90°). The desquamating apical cytoplasm (*) may be the expression of apocrine secretion. The peripheral surface is similar to the cell surface in the central region of the non-sensory epithelium in Fig. 44. *Ci*, Cilia. *Bar* 5 μm

Fig. 46. Surface view of three goblet cells from the peripheral region of the organ. Two of these seem to have secreted a large amount of mucous (*mu*) and have holes in the apical cytoplasm (*), whereas another cell seems to be at the begining of the secretory process (*arrow*). *Bar* 5 μm

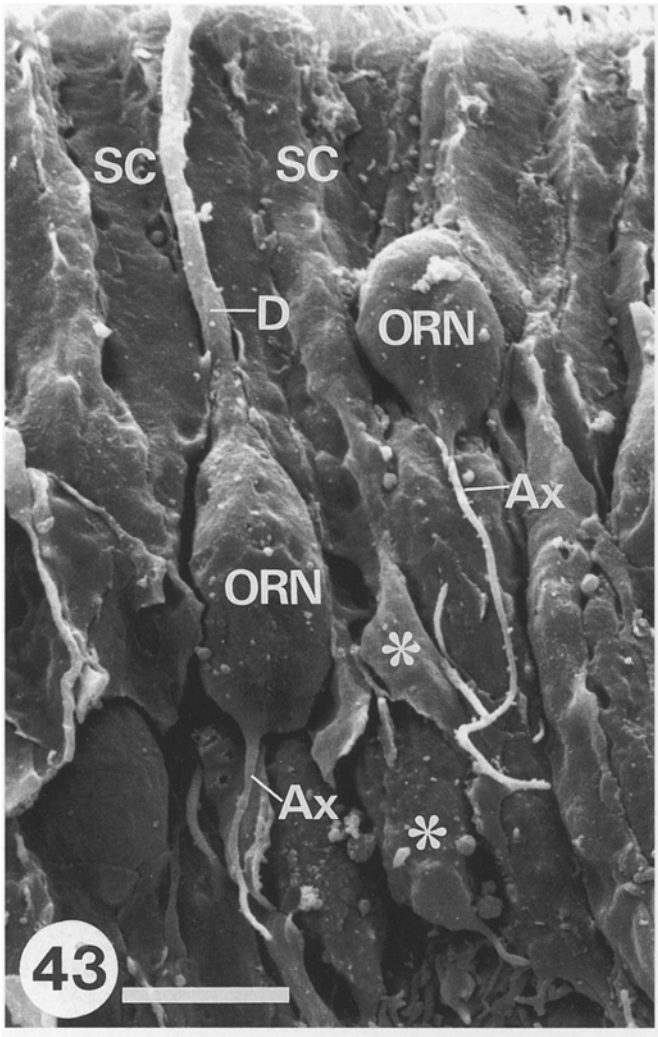
SC
SC
D
ORN
Ax
ORN
Ax
43

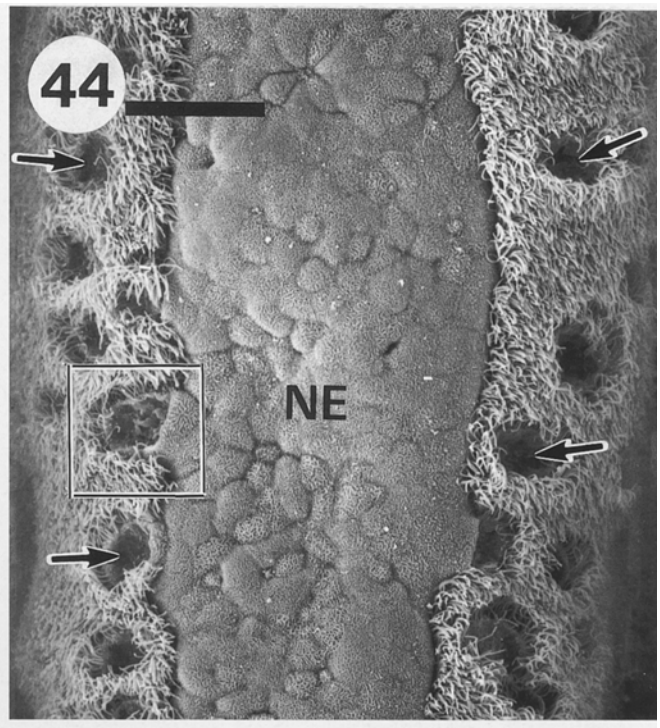
44
NE

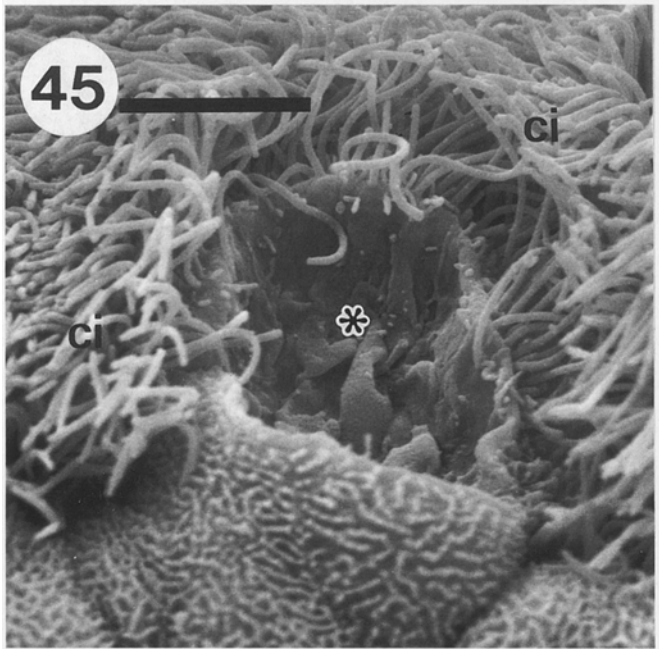
45
ci
ci

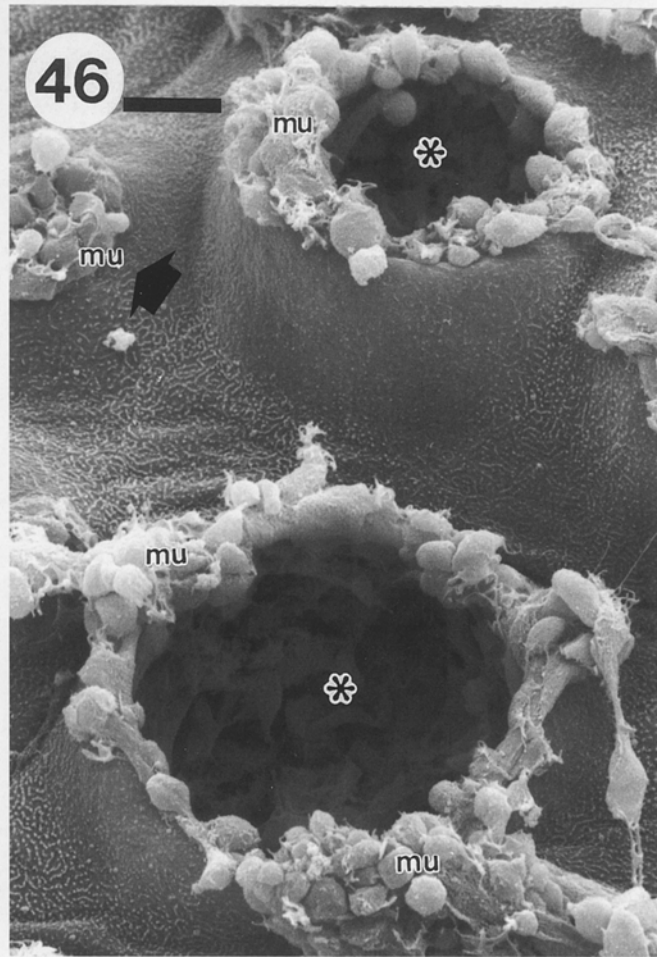
46
mu
mu
mu
mu

the sustentacular cells in their supranuclear region (Fig. 17), which is also rich in rER and free ribosomes (Fig. 28). Numerous smooth vesicles fill the supranuclear cytoplasm (Figs. 23, 24, 26), mixed with multivesicular bodies (Fig. 25), but secretory granules were never observed.

A basal part of the OE is shown in Fig. 29. The basal cells have less cytoplasm than the receptors or sustentacular cells; in the cytoplasm there are numerous polysomes but only a few mitochondria and a small Golgi complex. Just above the basal cells are elements with a dark, lobulated nucleus, a dense chromatin pattern and an electron-dense cytoplasm, and other cells with oval nuclei, numerous polysomes, and only sparse profiles of rER.

The peripheral region and the free endings of the lamellae of the OO are covered with a non-sensory epithelium. Three paraplast sections stained with Alcian blue are shown in Figs. 30–32. Many goblet cells with Alcian blue-positive granules are illustrated in the section from the periphery of the OO (Fig. 30), while longitudinal sections of the dorsal (Fig. 31) and ventral parts (Fig. 32) of the lamellae are also shown. Some goblet cells seem to have secretory granules extruding from their apical poles, and a mucus layer can be seen on the free surface of this epithelium. Cells with lightly stained, oval nuclei and voluminous Alcian blue-negative cytoplasm are mixed with the Alcian blue-positive goblet cells (Figs. 30–32). Isolated goblet cells can also been seen in the OE (Figs. 31, 32). Epoxy sections show more details of the goblet cells (Fig. 33) which are numerous in the epithelium of the peripheral region of the OO, and have secretory granules of variable density (Fig. 33). TEM micrographs of this region are shown in Figs. 34–36. Most goblet cells have basal nuclei with a dense chromatin pattern (Figs. 34, 35), while in the supranuclear region there is a prominent rER complex and a Golgi complex formed by small cisternae (Fig. 37). Isolated goblet cells are also present in the OE proper (Figs. 20, 37). Near the goblet cells are "light cells" characterized by small, lobulated nuclei with a light chromatin pattern and one or two nucleoli (Figs. 34, 36). Secretory granules were not observed in the cytoplasm of the "light cells" (Figs. 35, 36). Putative immune system cells are accumulated in the peripheral region of the OO (Figs. 33, 34). Mitotic figures are occasionally seen among these cells (Fig. 34).

SEM observations serve to illustrate the three-dimensional organization of the skate OO. From the ventral region of the OO, each lamella shows three different surface patterns, whereas the olfactory sensory epithelium proper is distributed on the sides of each lamella, forming folds (Fig. 38). Figure 39 shows part of a fold at higher

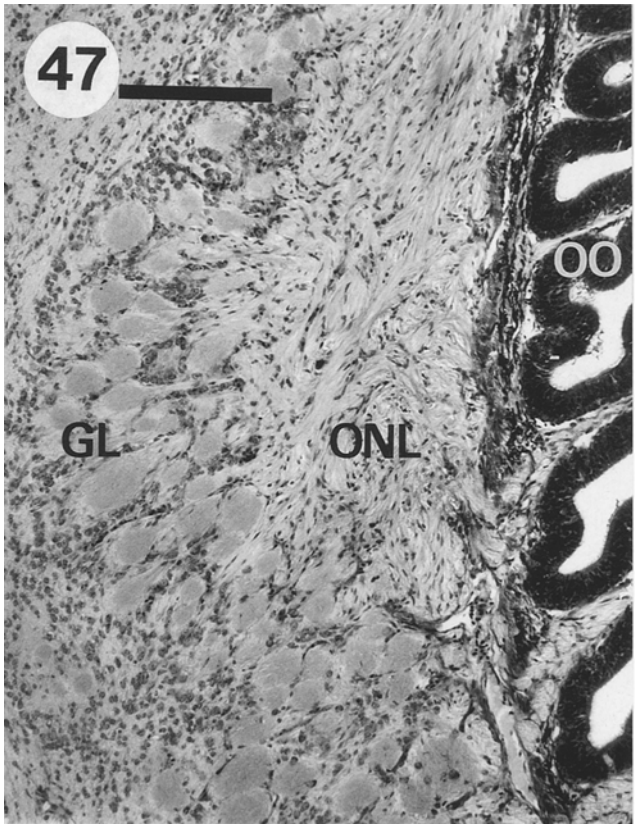

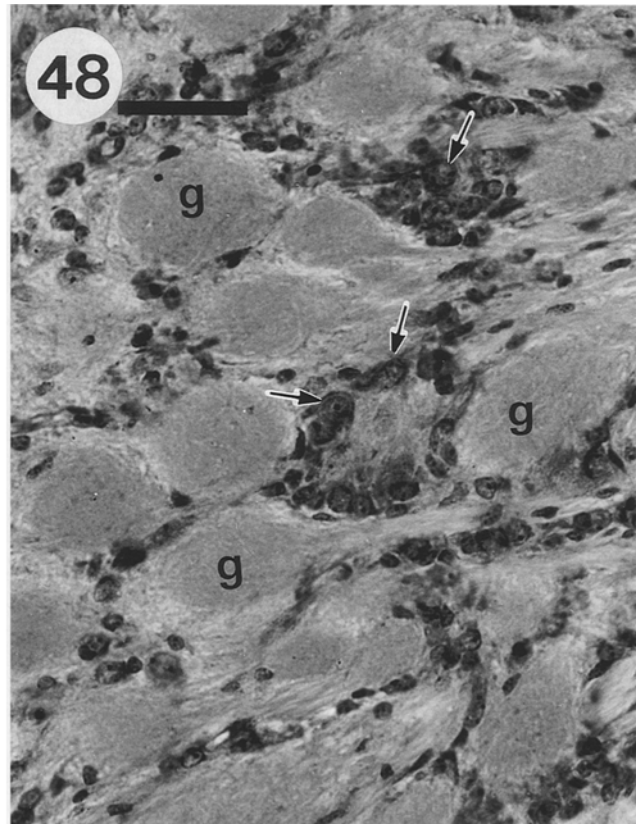

Fig. 47,48. Light micrographs of an olfactory bulb section stained with the Klüver-Barrera method

Fig. 47. Transverse section containing the olfactory bulb adjacent to the olfactory organ (*OO*). The glomerular layer (*GL*), where boundaries of individual glomeruli are clearly seen, is located next to the olfactory nerve layer (*ONL*). *Bar* 200 μm

Fig. 48. Higher magnification of the *GL*. Some of the largest cells of the *OB*, mitral cells (*arrows*), are present between the glomeruli (g). *Bar* 50 μm

magnification where a plexus of cilia of the sustentacular cells partially covers the apical poles of sparse goblet cells. Further higher power observation of the inside of the plexus of cilia revealed thinner processes underneath many cilia; these processes are microvilli of type 1 receptor neurons (Fig. 40). Observations on the lateral surface of the OE demonstrate dendritic knobs of type 1 receptor neurons. Figure 41 shows a dendritic knob of a type 1 neuron; it has many thin microvilli spread out between the cilia of sustentacular cells in a complicated pattern. The bulbar dendritic knob of type 2 receptor neurons is also observed in SEM specimens; this knob has a few thick microvilli that are thicker than the cilia (Fig. 42). Figure 43 shows neurons and sustentacular cells in the OE. The oval soma of a receptor neuron has two processes; the thicker one, reaching the luminal surface, can be recognized as a dendrite, whereas the thinner proximal process, reaching the basal portion of the epithelium, can be recognized as the axon. The free surface of each sustentacular cell is covered with cilia and short microvilli (Fig. 41), whereas its proximal region is complicated by foot processes (Fig. 43).

The surface morphology of the non-sensory epithelium is shown in Figs. 38 and 44–46. Every lamella shows hemispherical cell surfaces covered with short, stubby microvilli (Fig. 44). This surface changes to a ciliated one through a transitional zone where round holes can be seen (Figs. 38, 44). A high-power picture demonstrates that the holes are caused by the apocrine secretion of goblet cells (Fig. 45), shown also in the peripheral region of the OO (Fig. 46).

A tubular OB is located adjacent to the OO. Upon entering the OB, the axons of the olfactory receptor neurons form well-defined glomeruli (Fig. 47), and at their immediate periphery there are large, putative mitral cells (Fig. 48).

Discussion

The OE of *Raja eglanteria* contains two morphologically identifiable types of olfactory receptor neurons (named type 1 and type 2), ciliated sustentacular cells, and basal cells. The surface of the OE is covered with a layer of mucus produced by goblet cells located mainly in the non-sensory region of the OO. In this species, we did not recognize Bowman's glands, a typical secretory structure common in terrestrial vertebrates.

Both types of olfactory receptors described here have microvilli on their free dendritic endings and some basal bodies in the distal region of the dendrite, but no true cilia. These results are consistent with the observations of others for chondrichthian fishes such as ratfish (Holl 1973), sharks (Reese and Brightman 1970; Bronshtein 1976; Theisen et al. 1986; Zeiske et al. 1986), and rays (Bronshtein 1976). Thus, the lack of cilia in chondrichthians may be a general morphological characteristic, and the microvilli are the only device apt to extend the free receptor membrane; lack of cilia calls into question the *specific* role of these organelles in the odor-detection mechanism (Graziadei and Tucker 1970). Combining TEM and SEM, we have described a novel type of olfactory receptor (type 2 neuron) identified by *stiff microvilli*, a larger and shorter dendrite, and characteristic organelle content. The large bipolar cells observed with the Golgi method (Fig. 9 D, E) may correspond to type 2 sensory neuron, but observations indicate that neither type 1 nor type 2 has a specific spatial pattern of distribution, as they both appear in all regions of the epithelium. However, it will be necessary to conduct a morphometric analysis to clarify the ratio and distribution pattern of the two types of receptors.

Rod-shaped dendritic endings were first described by Bannister (1965) in the olfactory epithelium of a teleost, the minnow *Phoxinus phoxinus*. These dendritic endings extend a naked rod with a single or double point in the the luminal surface and contain three or more bundles of closely packed filaments and small vesicles. The internal structure of these rod-shaped endings has some similarity with the dendritic knobs of the type 2 receptors in the skate OE. Ichikawa and Ueda (1977) and Yamamoto (1982) have also reported rod-shaped dendritic endings. None of the previous authors, however, have described the morphology of the perikarya of the rod-shaped putative receptors or their microvilli at an ultrastructural level, thus a precise comparison cannot be made with our stiff microvillar receptors. It will be of interest to study the distribution of these new receptors in other elasmobranch fishes to determine their spatial arrangement, distribution across species, and eventually their functional significance.

The Golgi studies have revealed a polymorphic population of sustentacular cells; some have processes reaching the basement membrane of the OE, whereas the proximal processes of others branch in the upper two thirds of the OE (Rafols and Getchell 1983). A common feature of skate sustentacular cells is the presence of motile cilia displaying a 9+2 axonemal structure with obvious dynein arms. Each cilium displays a prominent rootlet and subrootlet system surrounded by numerous mitochondria. Secretory granules, which are obvious in sustentacular cells in the OE of other vertebrates (see for example Graziadei 1971, 1973), are not present in sustentacular cells of the skate OE. These morphological characteristics suggest that the major role of sustentacular cells of the skate OE is to disperse the mucus on the free epithelial surface and, probably, the odorants by ciliary synchronous beat, a mechanism that does not seem necessary in nonaquatic animals. The cilia and a prominent rootlet system are, indeed, characteristic of many chondrichthians (Reese and Brightman 1970; Holl 1973; Bronshtein 1976; Theisen et al. 1986; Zeiske et al. 1986). In agreement with our observations, presumptive secretory granules have not been reported in sharks, but Theisen et al. (1986) did report the presence of small vesicles in the apical regions of the sustentacular cells (in the catshark), and these authors characterized them as "secretory vesicles". In teleosts, microvilli and secretory granules of sustentacular cells in the OE seem to be the norm (Bannister 1965; Ichikawa and Ueda 1977; Zeiske et al. 1976; Delfino et al. 1981; Yamamoto 1982; Cancalon 1983). Ciliated sustentacular cells in the OE seem to be characteristic of the chondrichthian fish.

Reese and Brightman (1970) described sparse goblet cells in the OE of nurse sharks and guitar fish. In agreement with the results of Theisen et al. (1986), numerous goblet cells arranged in preferential locations were observed in the skate. For example, clusters of these cells are abundant in the peripheral part of the OO and are sparse among the olfactory receptor neurons. Apocrine and holocrine secretion, which is more vigorous in the non-sensory regions, was apparent. The morphological observations suggest an active secretion of mucus. In the regions of more abundant goblet cells, "light cells", which we have interpreted as immature stages of the goblet cells, were observed. Efficient renewal of goblet cells may help maintain a steady production of a product that plays an important role in perireceptor events (Getchell et al. 1984; Carr et al. 1990). An ancillary function of the mucus layer may be as a defence against bacterial infections.

The skate OE has the basic cell types observed throughout the vertebrates, but with some specific differences. The receptors lack cilia, but the sustentacular cells have cilia as a constant feature. Although specific autoradiographic studies remain to be implemented, the presence of mitotic figures among the basal cell population in the skate is an indication of a dynamic population of olfactory receptor neurons as demonstrated in several other vertebrate classes (for reviews, see Graziadei 1977, 1990; Graziadei and Monti Graziadei 1985).

The present results are a first attempt to describe the basic morphology of the OO of a skate (*Raja eglanteria*) and to characterize its cellular components. The availability of procedures, mentioned above, that permit the captive breeding and rearing of embryos and offspring in the laboratory under strict environmental conditions will allow the use of this animal for a variety of embryological studies, and for the study, more specifically, of its olfactory system. We have also documented that in *Raja*, as in other elesmobranchs (Dryer and Graziadei 1993), the OB has a characteristic elongated shape and is intimately adjacent to the OO; the OB and OO are connected by short filaments of the olfactory nerve. This feature is an ideal morphological characteristic for the study of primary sensory projections into the brain (see Dryer and Graziadei 1994).

Acknowledgements. We wish to express our gratitude to Ms. Kim Riddle, Sandra Silvers and Annette Black for their technical assistance in electron microscopy. We thank Mr. Charles Badland for helping with the photographic work and Ms. Mika Takami for her invaluable assistance in the preparation of this manuscript. This work was supported by grants from the National Institutes of Health to P. P. C. G. (NS 20699 and DC 01071) and from Walt Disney Imagineering to C. A. L.

References

Anholt RRH (1987) Primary events in olfactory reception. Trends Biochem Sci 12:58–62

Bannister LH (1965) The fine structure of the olfactory surface of teleostean fishes. Q J Microsc Sci 106:333–342

Bronshtein AA (1976) Fine structure of the elasmobranch (elasmobranchii) olfactory organ. Zh Évol Biokhim Fiziol 12:63–67

Cancalon P (1983) Receptor cells of the catfish olfactory mucosa. Chem Senses 8:203–209

Carr WES, Gleeson RA, Trapido-Rosenthal HG (1990) The role of perireceptor events in chemosensory processes. Trends Neurosci 13:212–215

Delfino G, Bianchi S, Ercolini A (1981) On the olfactory epithelium in cyprinids: a comparison between hypogean and epigean species. Ital J Zool [Suppl] 14:153–180

Dryer L, Graziadei PPC (1993) A pilot study on morphological compartmentalization and heterogeneity of the elasmobranch olfactory bulb. Anat Embryol 188:41–51

Dryer L, Graziadei PPC (1994) Mitral cell dendrites: a comparative approach. Anat Embryol 189:91–106

Eisthen HL (1992) Phylogeny of the vomeronasal system and of receptor cell types in the olfactory and vomeronasal epithelia of vertebrates. Microsc Res Tech 23:1–21

Getchell TV (1986) Functional properties of vertebrate olfactory receptor neurons. Physiol Rev 66:772–818

Getchell TV, Margolis FL, Getchell ML (1984) Perireceptor and receptor events in vertebrate olfaction. Prog Neurobiol 23:317–345

Graziadei PPC (1971) Topological relations between olfactory neurons. Z Zellforsch Mikrosk Anat 118:449–466

Graziadei PPC (1973) The ultrastructure of vertebrates olfactory mucosa. In: Friedmann I (ed) The ultrastructure of sensory organs. North-Holland, Amsterdam, pp 269–305

Graziadei PPC (1977) Functional anatomy of the mammalian chemoreceptor system. In: Müller-Schwarze D, Mozell MM (eds) Chemical signals in vertebrates. Plenum Press, New York, pp 435–454

Graziadei PPC (1990) Olfactory development. In: Coleman JR (ed) Development of sensory systems in mammals. John, New York, pp 519–566

Graziadei PPC , Monti Graziadei GA (1985) Neurogenesis and plastisity of the olfactory sensory neurons. In: Hope for a new neurology. Ann N Y Acad Sci 457:127–142

Graziadei PPC, Monti-Graziadei (1992) The influence of the olfactory placode on the development of the telencephalon in *Xenopus laevis*. Neuroscience 46:617–629

Graziadei PPC, Tucker D (1970) Vomeronasal receptors in turtles. Z Zellforsch Mikrosk Anat 105:498–514

Holl A (1973) Feinstruktur des Riechepithels von *Chimaera monstrosa* (Holecepheli). Mar Biol 23:59–72

Ichikawa M, Ueda K (1977) Fine structure of the olfactory epithelium in the goldfish, *Carassius auratus*. Cell Tissue Res 183:445–455

Lancet C (1986) Vertebrate olfactory reception. Ann Rev Neurosci 9:329–355

Luer CA (1989) Elasmobranchs (sharks, skates, and rays) as animal models for biomedical research. In: Woodhead AD, Vivirito K (eds) Nonmammalian animal models for biomedical research. CRC Press, Boco Raton, pp 121–147

Luer CA, Gilbert PW (1985) Mating behavior, egg deposition, incubation period, and hatching in the clearnose skate, *Raja eglanteria*. Environ Biol Fishes 13:161–171

Magrassi L, Graziadei PPC (1985) Interaction of the transplanted olfactory placode with the optic stalk and the diencephalon in *Xenopus laevis* embryos. Neuroscience 15:903–921

Meng Q, Yin M (1981) A study on the olfactory organ of skates, rays, and chimaeras. J Fish China 5:209–228

Monti Graziadei GA, Graziadei PPC (1984) The olfactory organ, neural transplantation. In: Sladek JR, Gash DM (eds) Neural transplants. Plenum Press, New York, pp 167–186

Rafols JA, Getchell TV (1983) Morphological relations between the receptor neurons, sustentacular cells and Schwann cells in the olfactory mucosa of the salamander. Anat Rec 206:87–101

Reese TS, Brightman MW (1970) Olfactory surface and central olfactory connexions in some vertebrates. In: Wolstenholme GEW, Knight J (eds) Taste and smell in vertebrates. Ciba Foundation Symposium. Churchill, London, pp 115–43

Stout RP, Graziadei PPC (1980) Influence of the olfactory placode on the development of the brain in *Xenopus laevis* (Daudin). I. Axonal growth and connections of the transplanted olfactory placode. Neuroscience 5:2175–2186

Takami S, Graziadei PPC (1991) Light microscopic study of mitral/tufted cells in the accessory olfactory bulb of the adult rat. J Comp Neurol 311:65–83

Takami S, Hirosawa K (1990) Electronmicroscopic observations on the vomeronasal sensory epithelium of a crotaline snake, *Trimeresurus flavoviridis*. J Morphol 205:45–61

Theisen B, Zeiske E, Breucker H (1986) Functional morphology of the olfactory organs in the spiny dogfish (*Squalus acanthias* L.) and the small-spotted catshark (*Scyliorhinus canicula* L.) Acta Zool 67:73–86

Yamamoto M (1982) Comparative morphology of the peripheral olfactory organ in teleosts. In: Hara TJ (ed) Chemoreception in fishes. Elsevier, Amsterdam, pp 39–59

Zeiske E, Caprio J, Gruber SH (1986) Morphological and electrophysiological studies on the olfactory organ of the lemon shark, *Negaprion brevirostris* (Poey). In: Uyeno T, Arai R, Taniuchi T, Matsuura K (eds) Indo-pacific fish biology: proceedings of the second international conference on indo-pacific fishes. Ichthyological Society of Japan, Tokyo, pp 381–391